Artificially Structured Superconductors

Loops, Boundaries and Interfaces

Manfred Sigrist

ETH Zürich

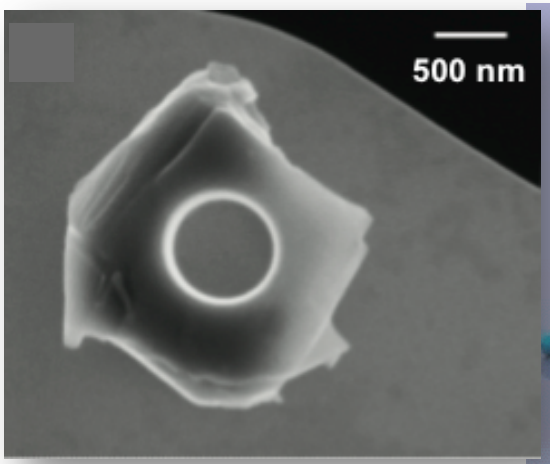

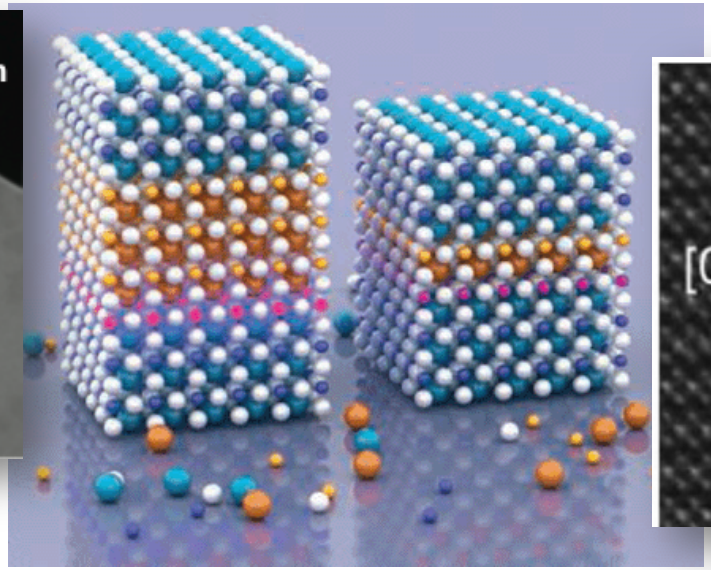

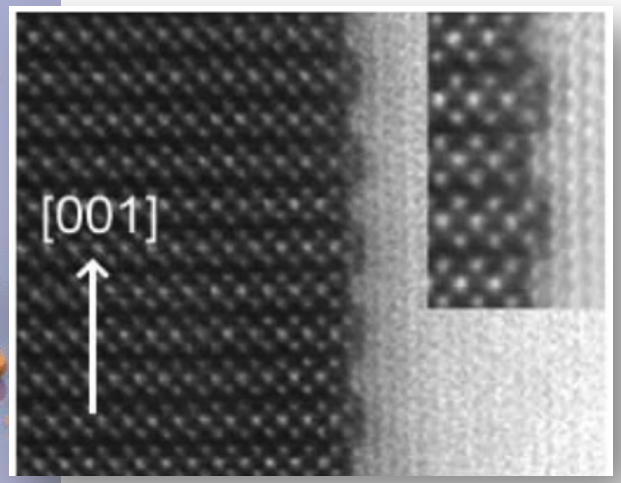

Artificially Structured Superconductors
Loops, Boundaries and Interfaces

Manfred Sigrist

ETH Zürich

- artificial structures:
  new properties and robustness of superconducting phases
- unconventional superconductivity in confined spaces
- spin-triplet superconductivity: d-vector manipulation

Artificially structured superconductors

Small devices give insights into the structure of the superconducting condensate

Little-Parks effect

$$\Phi_0 = \frac{hc}{2e}$$

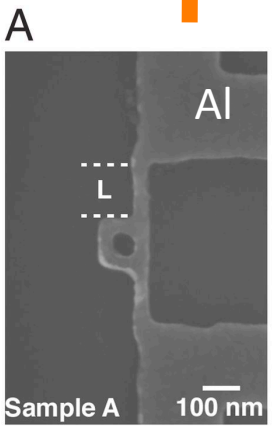

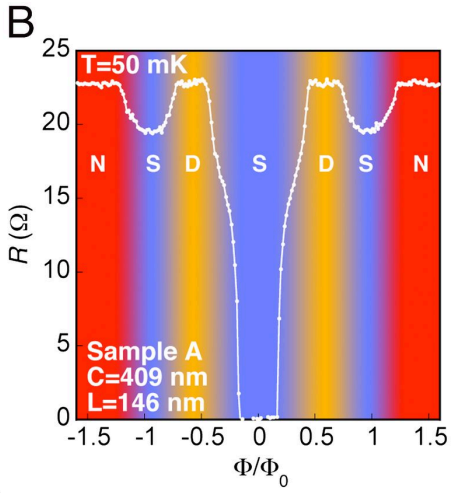

Staley & Liu (2012)

Josephson effect - SQUID

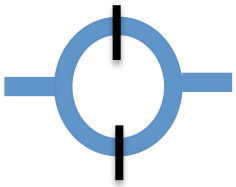

van Harlingen et al (1993)

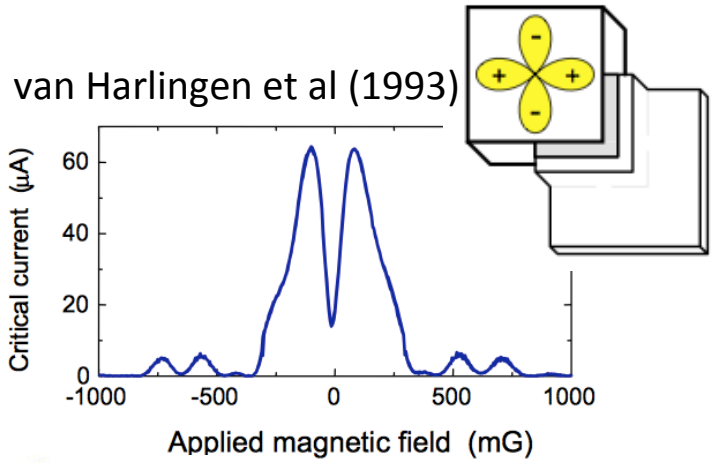

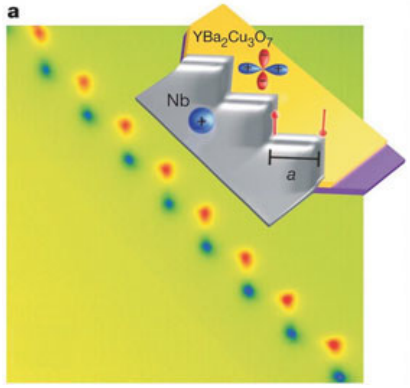

Hilgenkamp et al (2003)

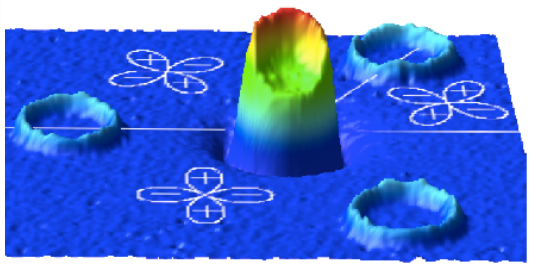

Tsuei, Kirtley et al (1994)

Superconducting heterostructures & superlatticies

Heterostructures / superlattices

$LaAlO_3$ / $SrTiO_3$

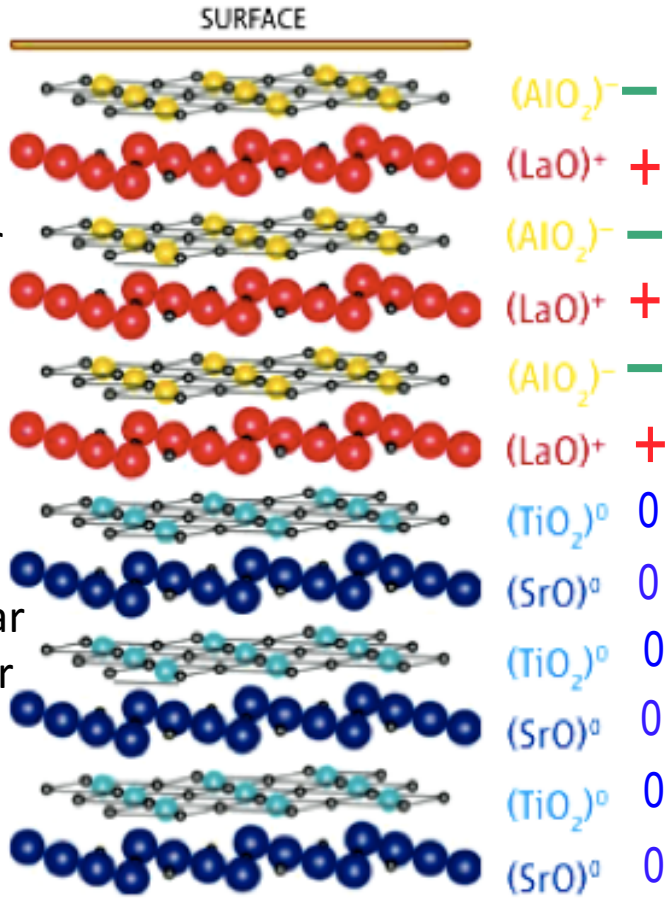

polar insulator

non-polar insulator

$LaAlO_3$

polar insulator

$SrTiO_3$

non-polar insulator

H.Y. Hwang group

Heterostructures / superlattices

$LaAlO_3$ / $SrTiO_3$

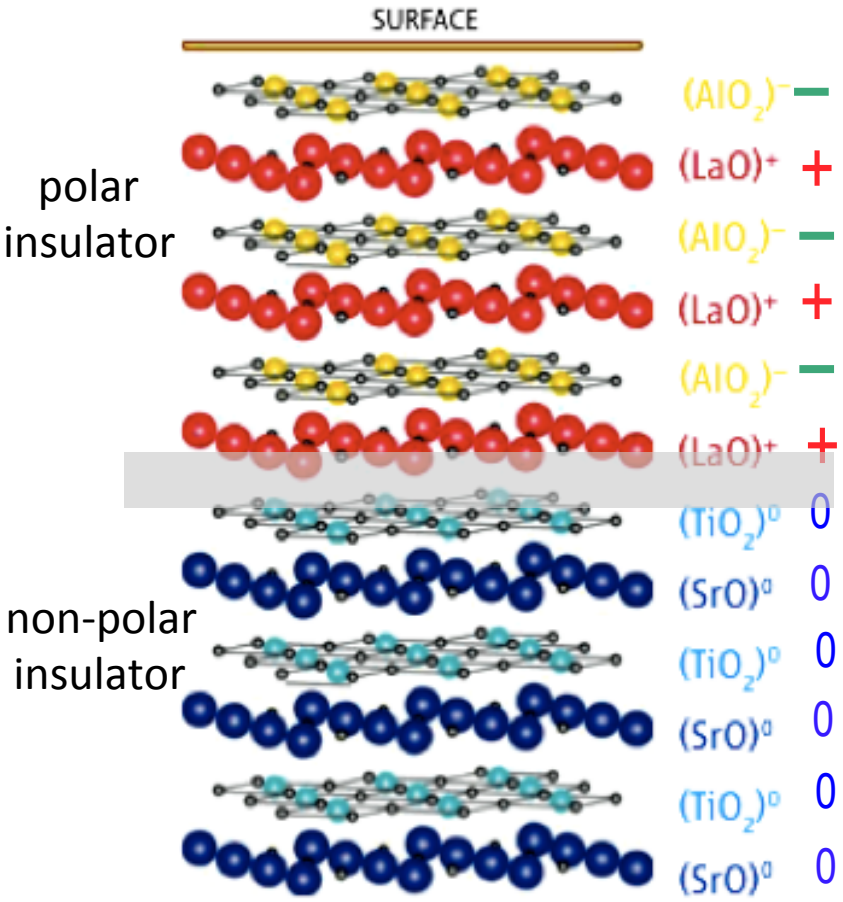

$LaAlO_3$ polar insulator

polar breakdown ?
2D metallic interface

$SrTiO_3$ non-polar insulator

H.Y. Hwang group

Heterostructures / superlattices

$LaAlO_3$ / $SrTiO_3$

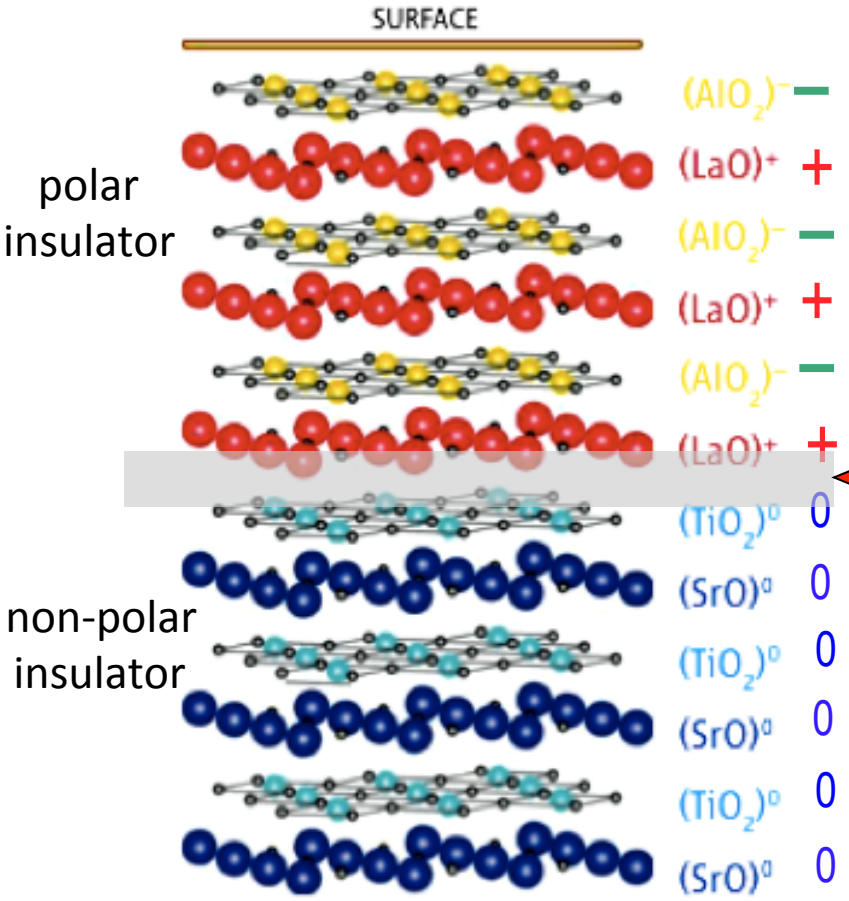

H.Y. Hwang group

interface superconductivity

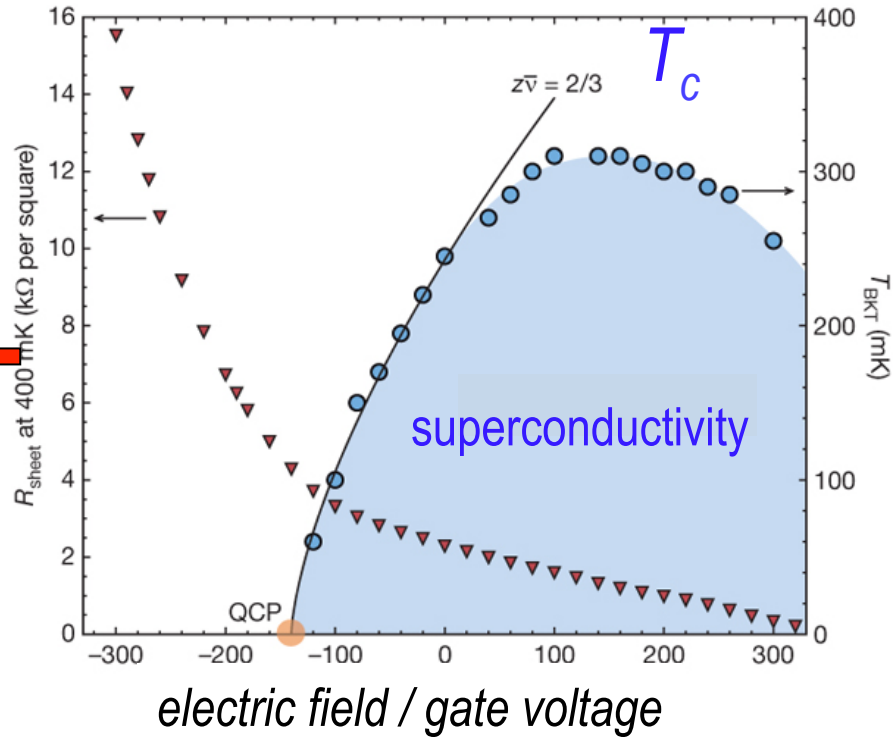

Reyren, Triscone, Mannhart et al.

Heterostructures / superlattices

$LaAlO_3$ / $SrTiO_3$

polar insulator

non-polar insulator

Spontaneous inplane ferromagnetism and inhomogeneity

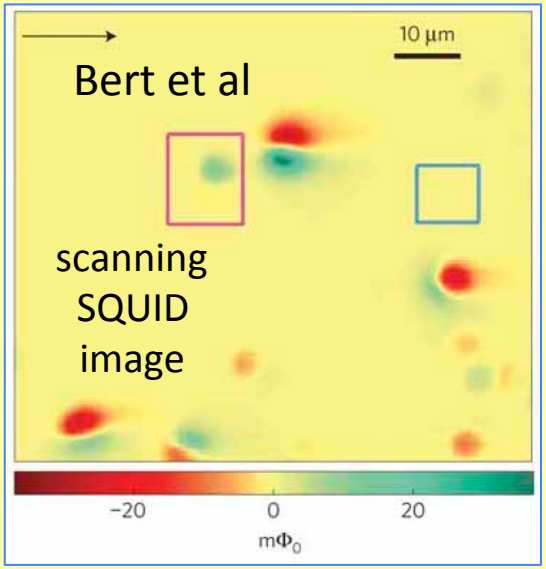

H. Hwang, K.A. Moler et al., R. Ashori et al.

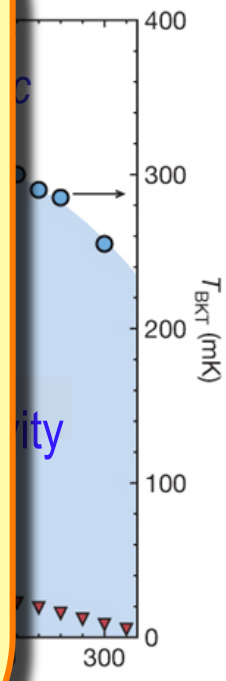

Reyren, Triscone, Mannhart et al.

H.Y. Hwang group

Heavy Fermion superconductors

$CeCoIn_5$

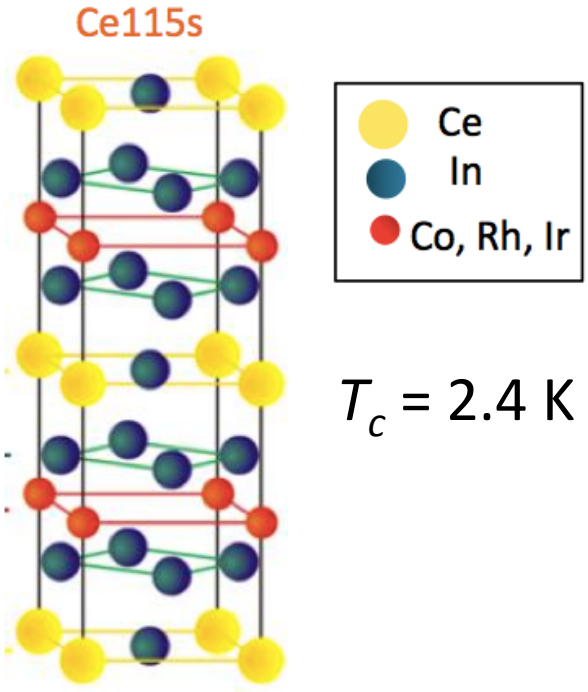

d-wave spin-singlet pairing

T_c = 2.4 K

Sarrao, Thompson et al

Heavy Fermion superconductors

$CeCoIn_5$

Ce115s

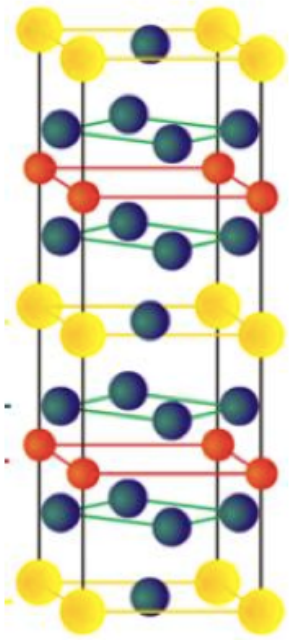

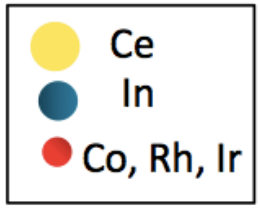

d-wave spin-singlet pairing

T_c = 2.4 K

paramagnetic limiting & "FFLO"

specific heat map

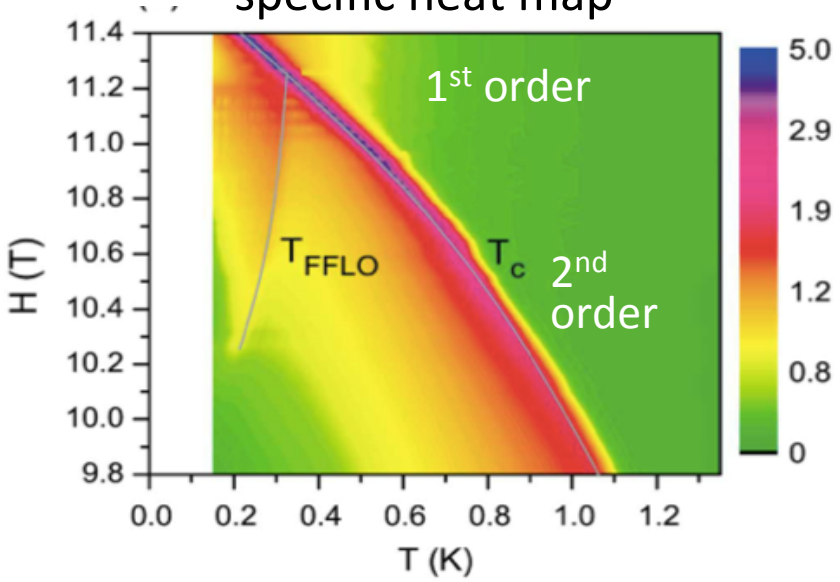

Sarrao, Thompson et al

Heavy Fermion superconductors

$CeCoIn_5$

Ce115s

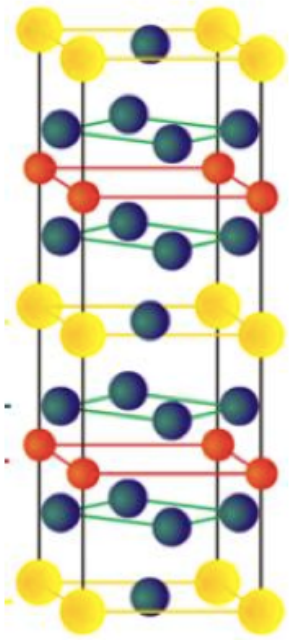

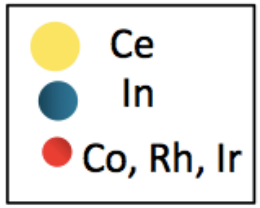

d-wave spin-singlet pairing

T_c = 2.4 K

Sarrao, Thompson et al

paramagnetic limiting & "FFLO"

specific heat map

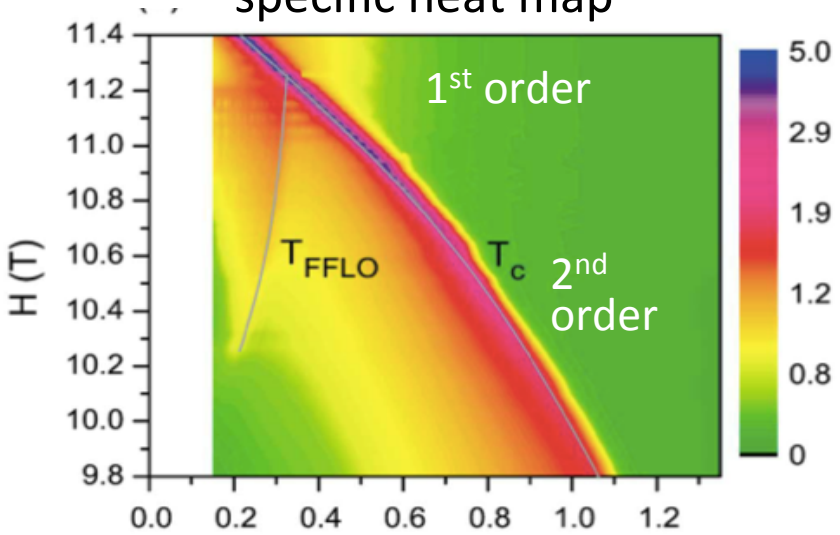

Maki parameter $\alpha = \sqrt{2}\frac{H_{c2}^0}{H_P}$

$$H_{c2}^0 = 0.7T_c \left.\frac{dH_{c2}}{dT}\right|_{T_c}$$

bulk $CeCoIn_5$

$$\alpha \approx 6$$

Heavy Fermion superconductors

$CeCoIn_5$

Ce115s

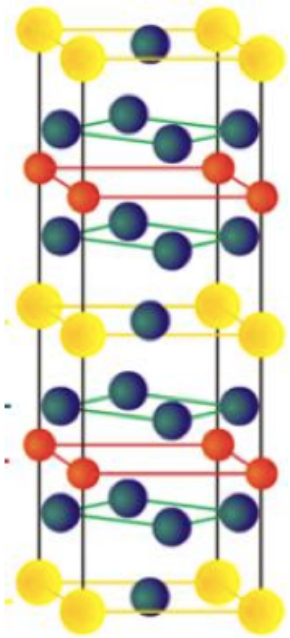

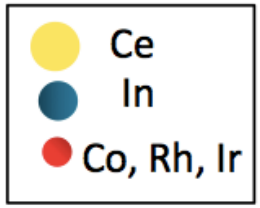

d-wave spin-singlet pairing

T_c = 2.4 K

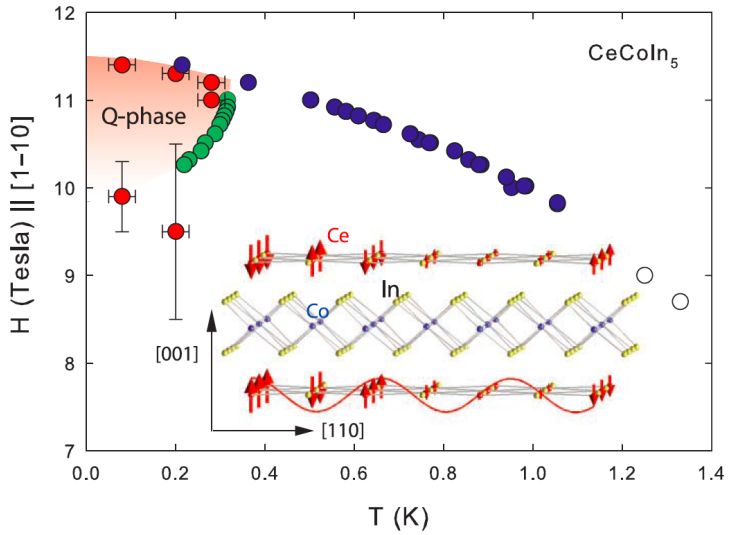

paramagnetic limiting & "FFLO"

specific heat map

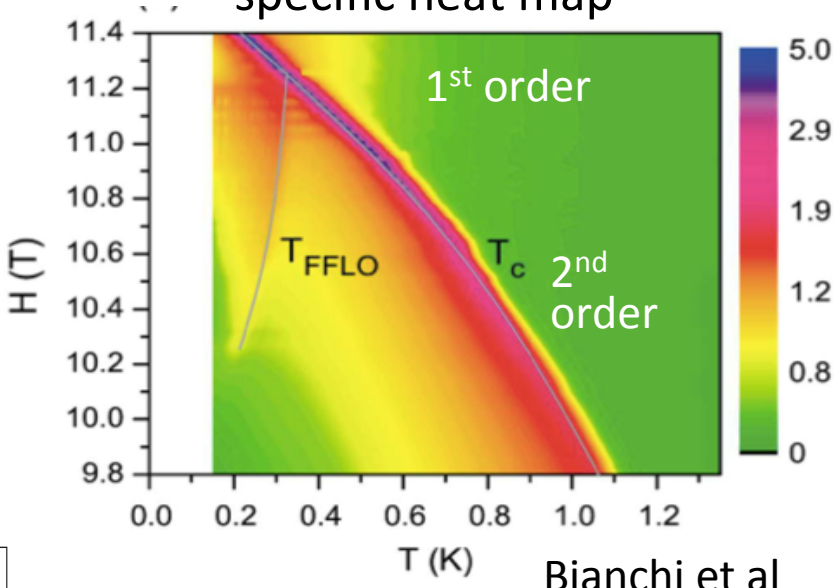

Bianchi et al

coexistence with incommensurate SDW

"Q-phase"

Curro et al
Kumagai et al } NMR

Kenzelmann et al neutron scattering

Heterostructures / superlattices

"towards a more 2D system"

$CeCoIn_5$ / $YbCoIn_5$

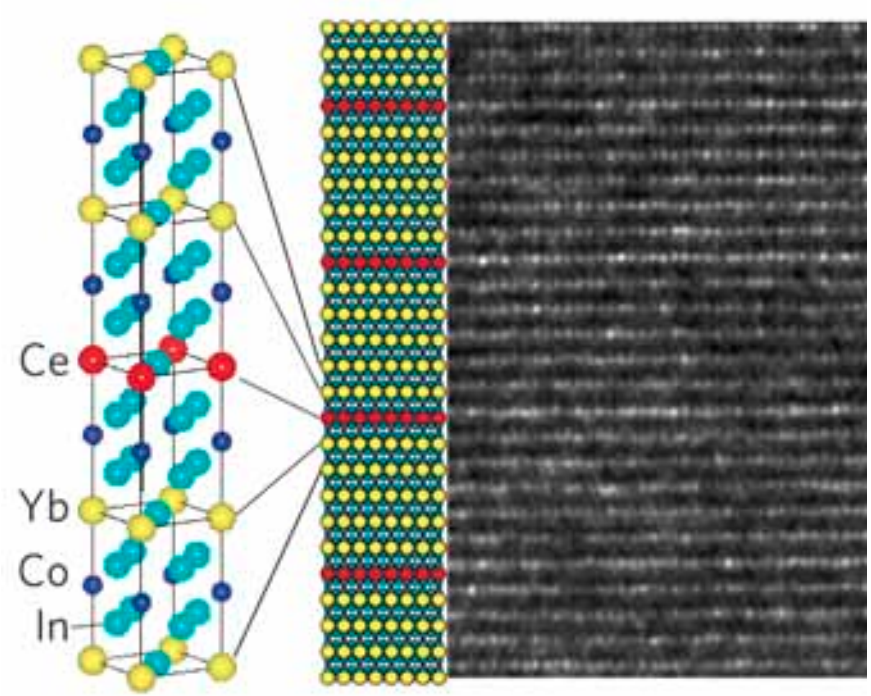

Matsuda & Shibauchi group (2011)

(Ce,Yb) = (*n*,*5*)

$CeCoIn_5$ heavy Fermion

$YbCoIn_5$ ordinary metal

Heterostructures / superlattices

"towards a more 2D system"

$CeCoIn_5$ / $YbCoIn_5$

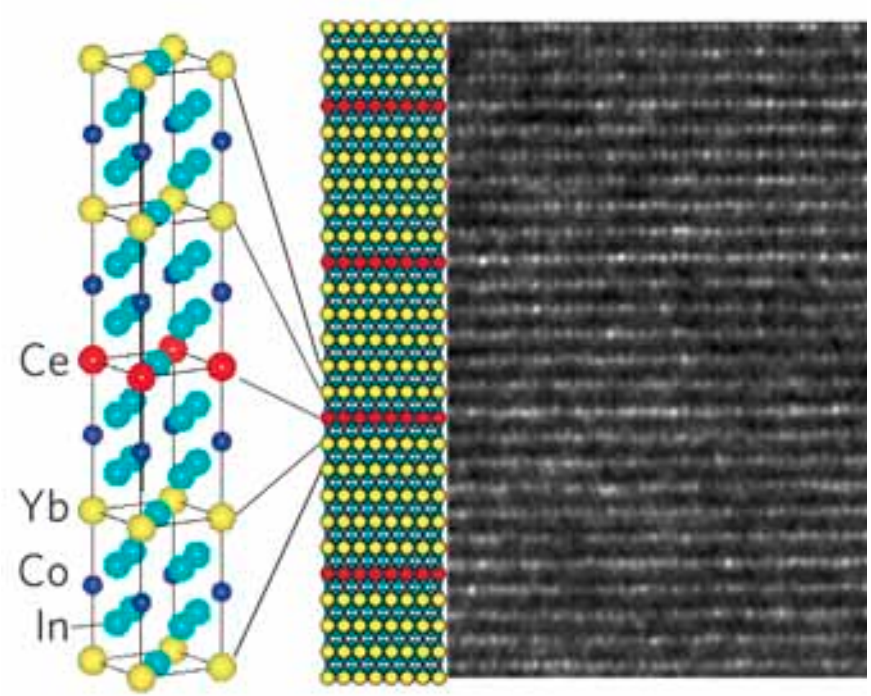

Matsuda & Shibauchi group (2011)

(Ce,Yb) = (*n*,*5*)

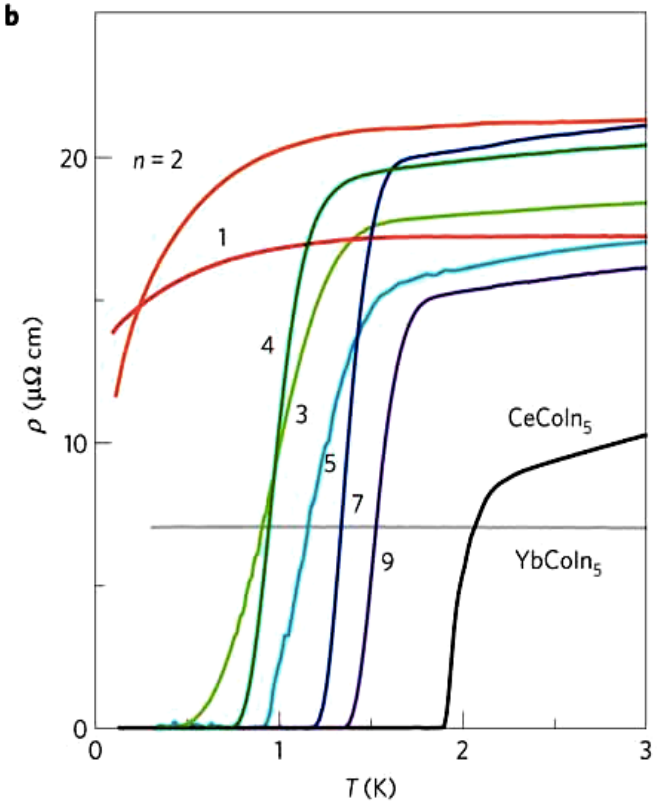

superconducting for

$$n \geq 3$$

Heterostructures / superlattices

"towards a more 2D system"

$CeCoIn_5$ / $YbCoIn_5$

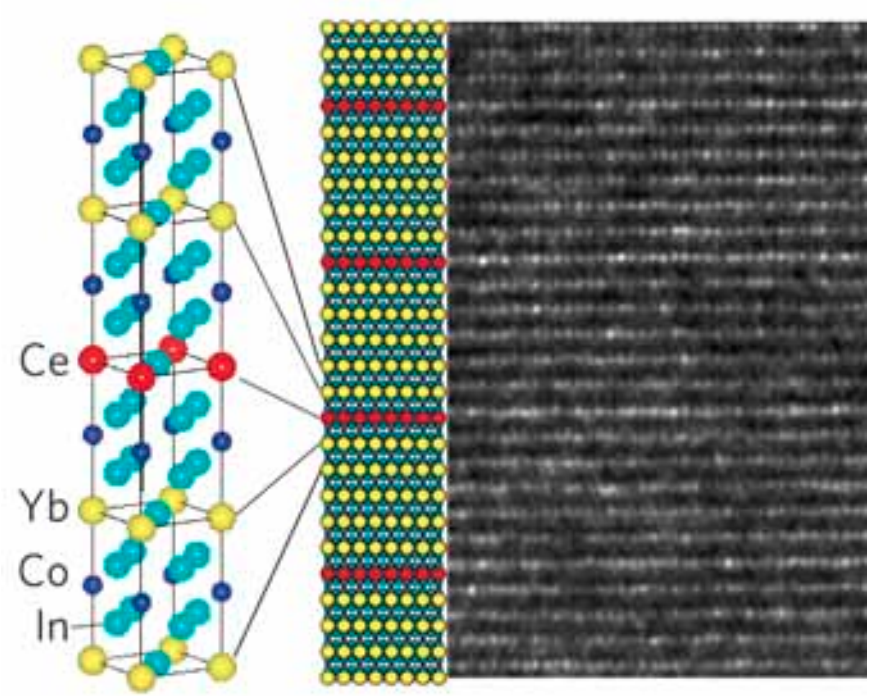

Matsuda & Shibauchi group (2011)

(Ce,Yb) = (*n*,*5*)

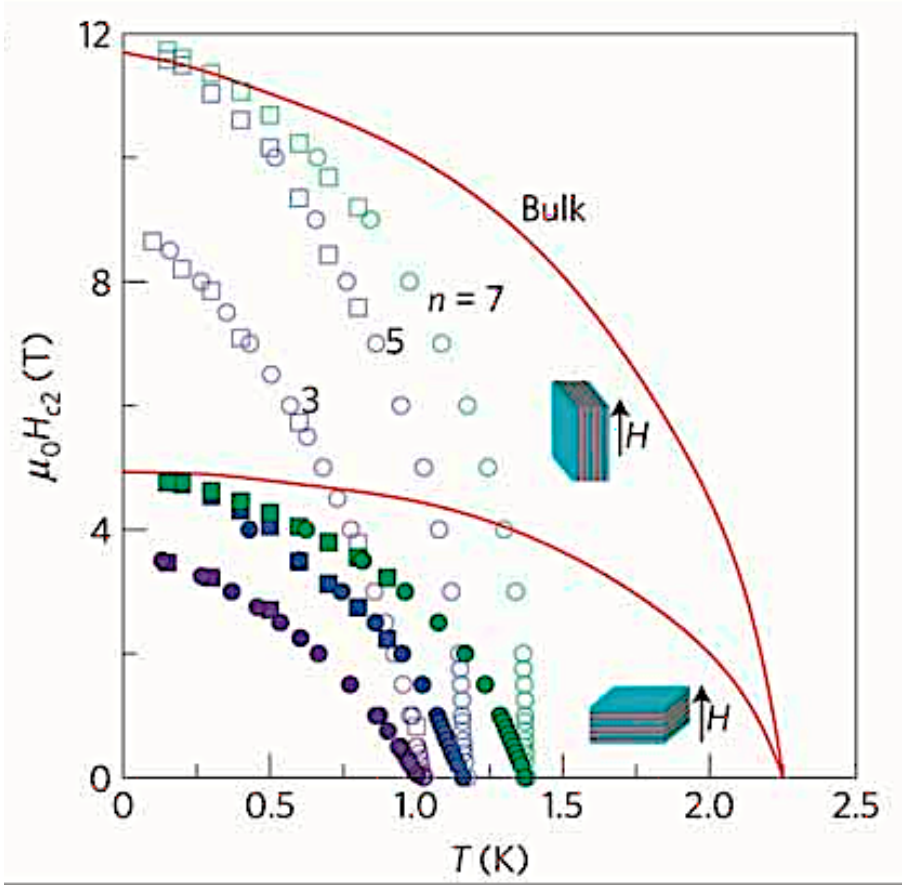

Non-centrosymmetricity

heterostructure

superlattice

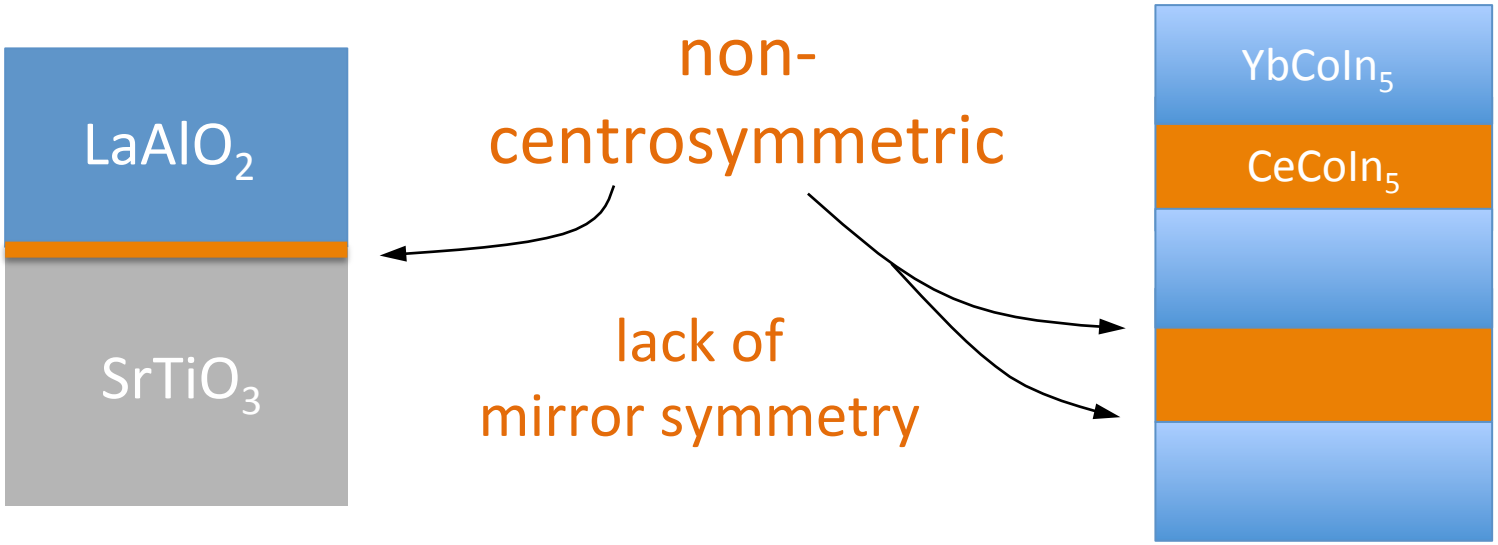

Rashba spin-orbit coupling

$$\mathcal{H} = \sum_{\boldsymbol{k},s} \epsilon_{\boldsymbol{k}} c^{\dagger}_{\boldsymbol{k}s} c_{\boldsymbol{k}s} + \alpha \sum_{\boldsymbol{k}} \sum_{ss'} \boldsymbol{g}_{\boldsymbol{k}} \cdot \boldsymbol{\sigma}_{ss'} c^{\dagger}_{\boldsymbol{k}s} c_{\boldsymbol{k}s'}$$

Non-centrosymmetric superconductors

Heavy Fermion superconductors

$CePt_3Si$

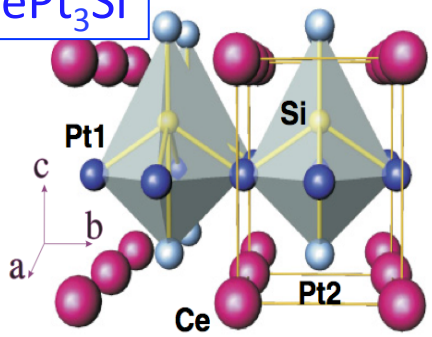

Bauer et al

$CeIrSi_3$

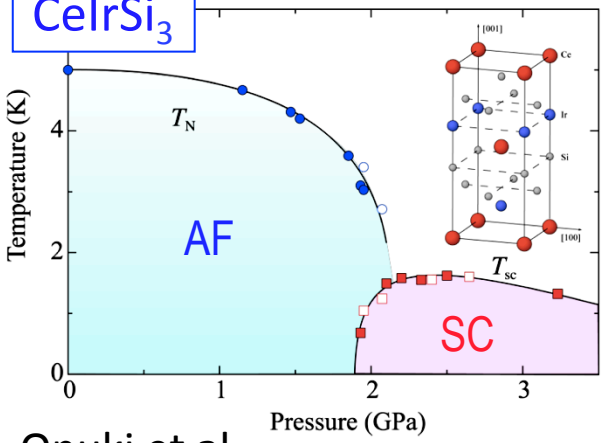

Onuki et al

Non-centrosymmetric superconductors

Heavy Fermion superconductors

$CePt_3Si$

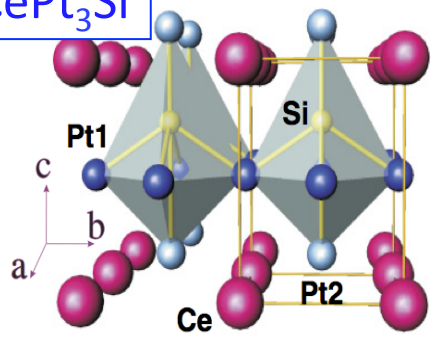

Bauer et al

$CeIrSi_3$

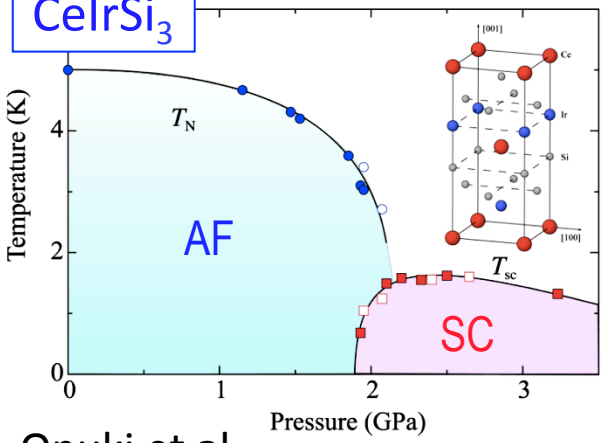

Onuki et al

spin susceptibility

^{29}Si-Knight shift

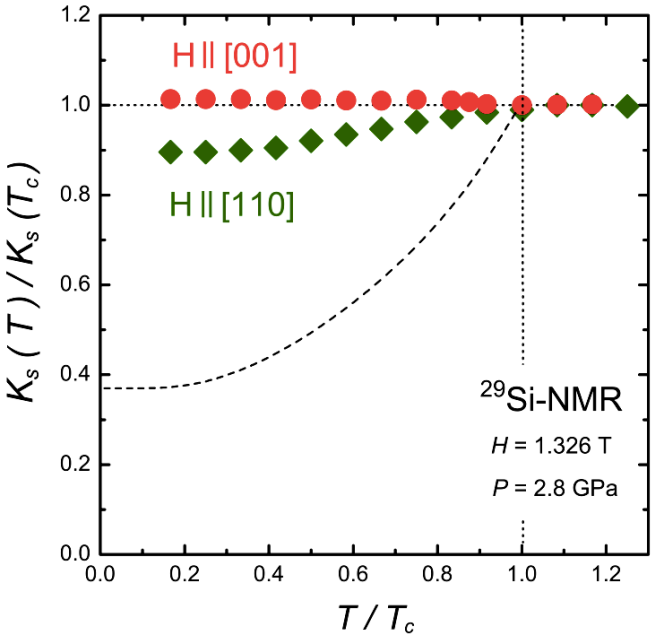

Mukuda et al

Non-centrosymmetric superconductors

Heavy Fermion superconductors

$CePt_3Si$

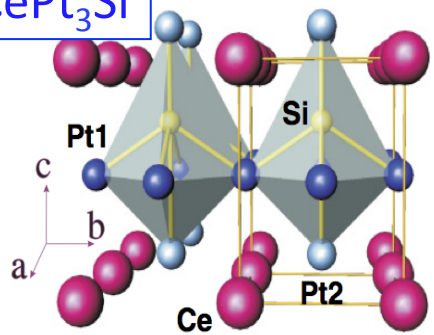

Bauer et al

spin susceptibility

^{29}Si-Knight shift

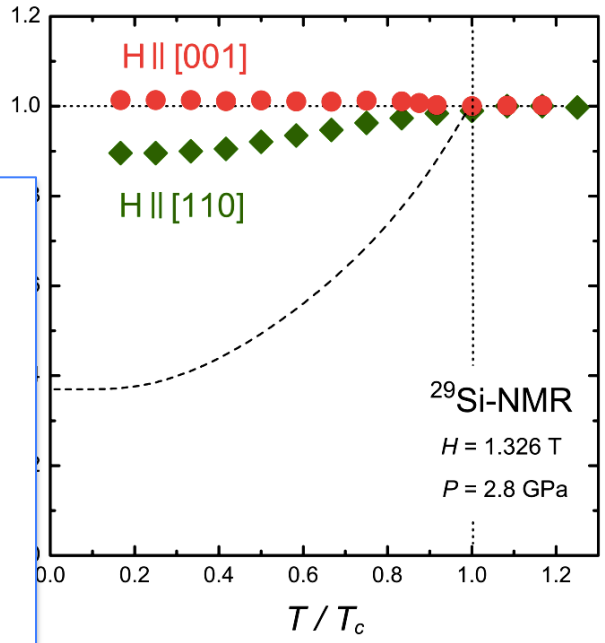

uda et al

Rashba spin-orbit coupling

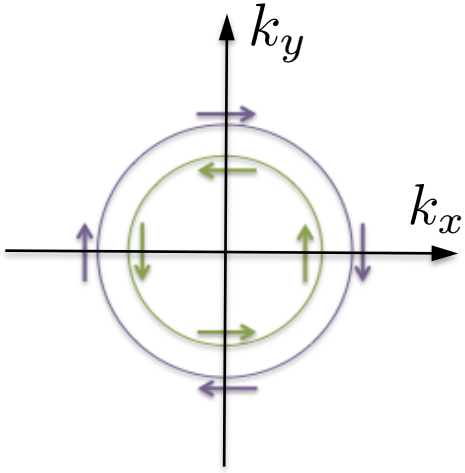

spin polarization
through
van Vleck effect

no pair breaking!

Non-centrosymmetric superconductors

Heavy Fermion superconductors

upper critical field

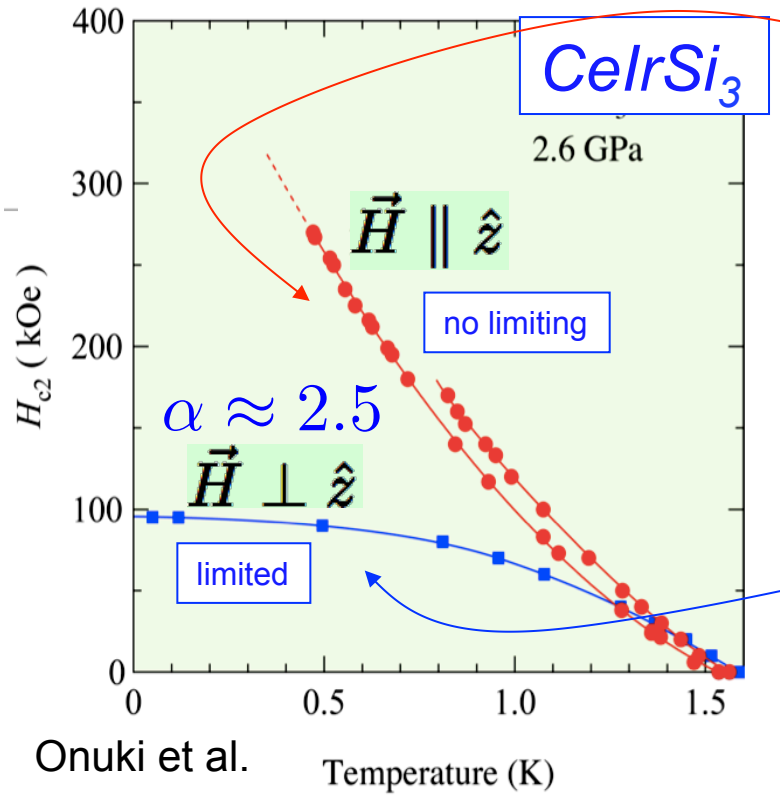

Onuki et al.

spin susceptibility

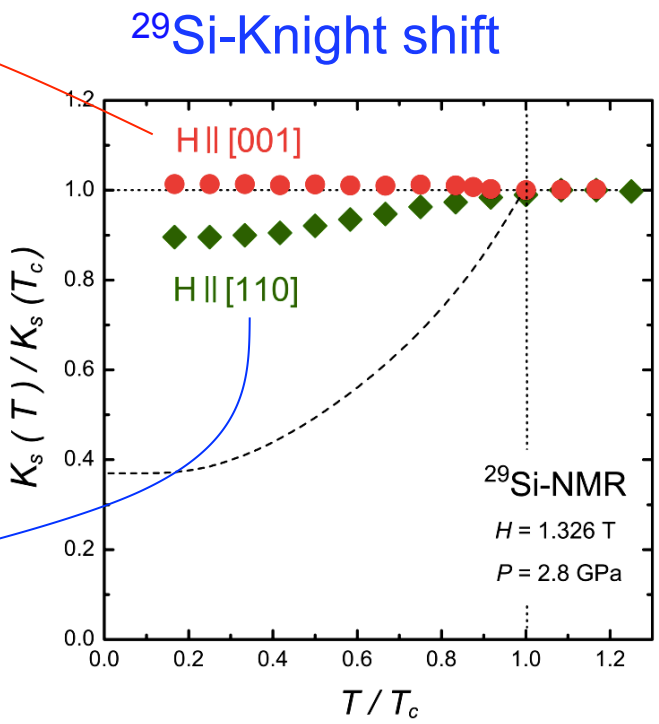

Mukuda et al

Non-centrosymmetric superconductors

Heavy Fermion superconductors

upper critical field

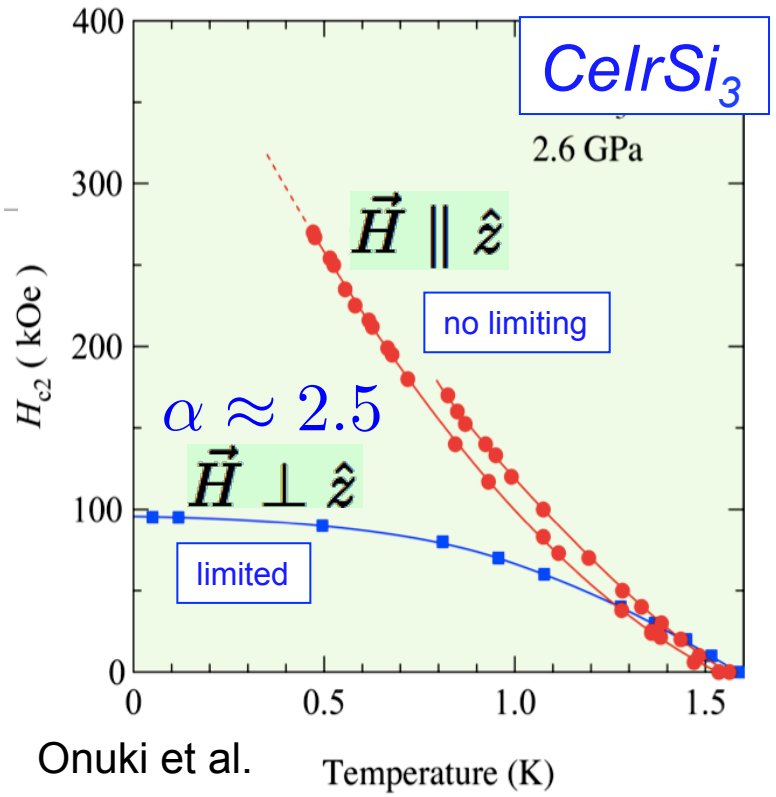

Onuki et al.

not heavy Fermion

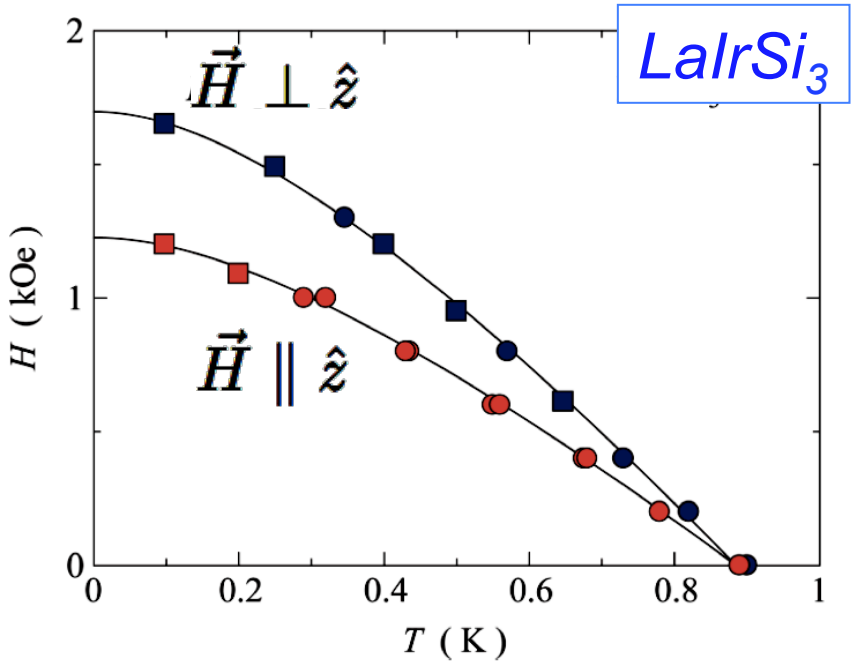

- 100 x smaller H_{c2}
- orbital depairing relevant

  light electrons ➡ large ξ

Heterostructure – LAO/STO

$LaAlO_3$ / $SrTiO_3$

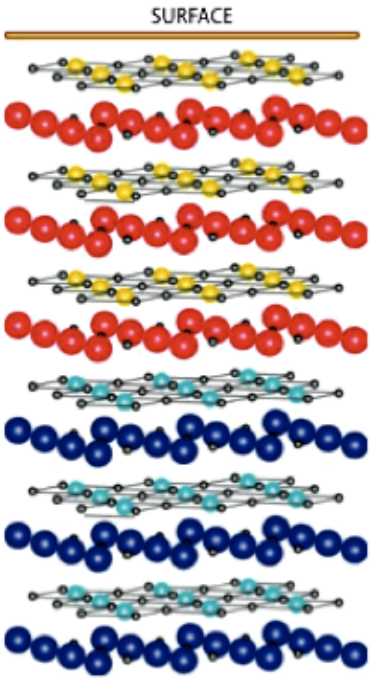

Does non-centrosymmetricity play a role for upper critical field?

Heterostructure – LAO/STO

$LaAlO_3$ / $SrTiO_3$

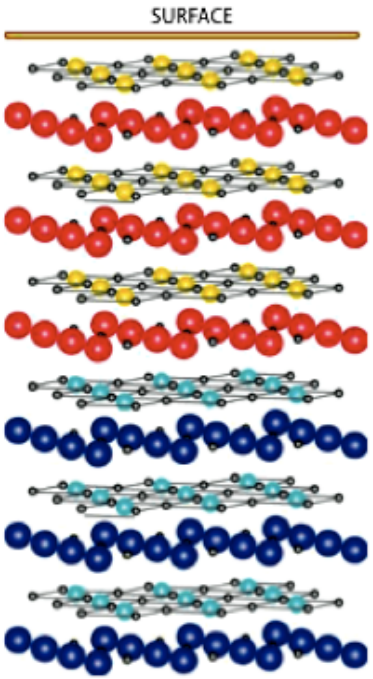

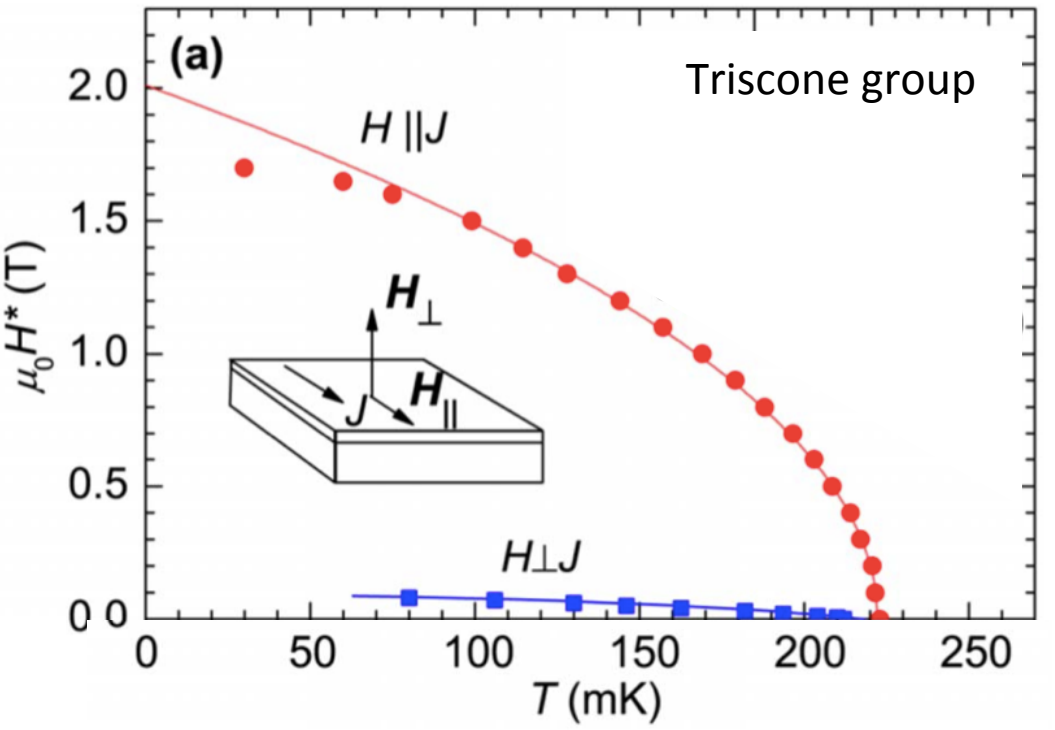

paramagnetic limiting field

$$H_p \sim \frac{\Delta_0}{\sqrt{2}\mu_B} \sim \frac{k_B T_c}{\mu_B} \sim 1 - 2T$$

Does non-centrosymmetricity play a role for upper critical field?

Superlattice – Ce115 / Yb115

$CeCoIn_5$ / $YbCoIn_5$

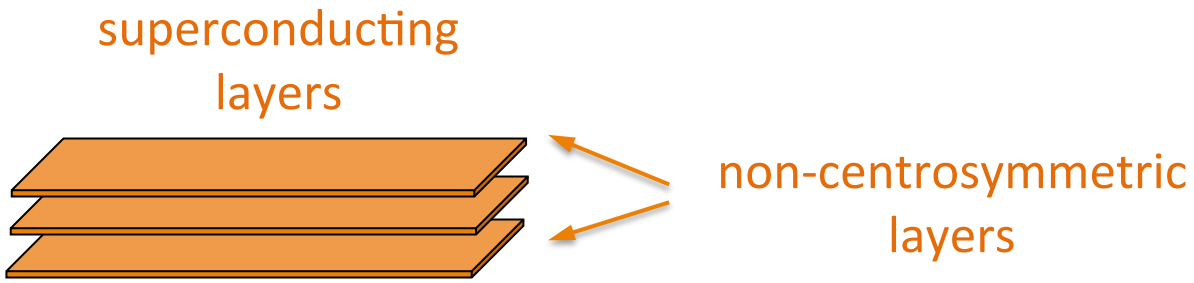

Superlattice – Ce115 / Yb115

$CeCoIn_5$ / $YbCoIn_5$

$$\alpha_1 = +\alpha \qquad \alpha_2 = 0 \qquad \alpha_3 = -\alpha$$

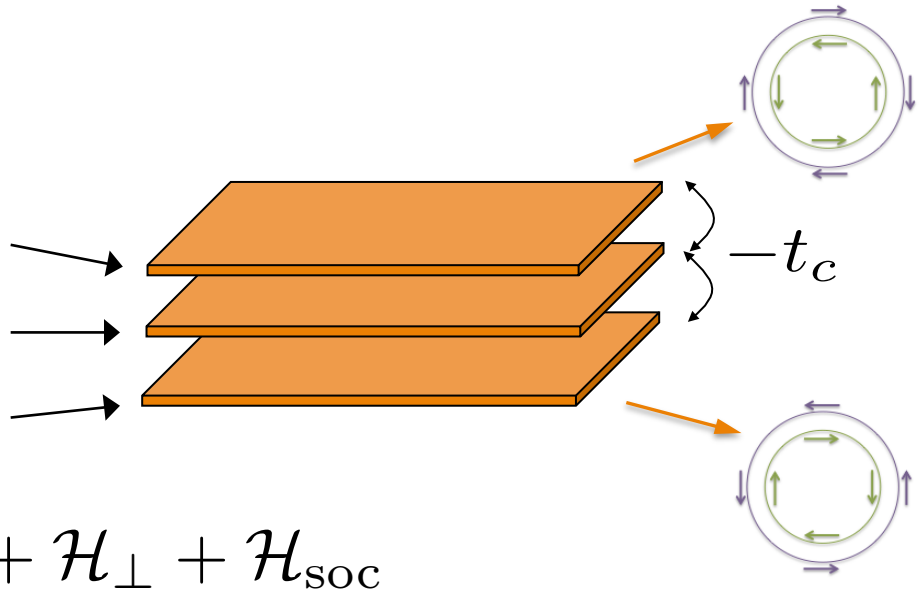

$$\mathcal{H} = \mathcal{H}_{\parallel} + \mathcal{H}_{\perp} + \mathcal{H}_{\rm soc}$$

$$\mathcal{H}_{\parallel} = \sum_{l=1,2,3} \sum_{\boldsymbol{k},s} \epsilon_{\boldsymbol{k}} c^{\dagger}_{\boldsymbol{k}ls} c_{\boldsymbol{k}ls}$$ intra-layer

$$\mathcal{H}_{\perp} = -t_c \sum_{\boldsymbol{k},s} \left\{ c^{\dagger}_{\boldsymbol{k}1s} c_{\boldsymbol{k}2s} + c^{\dagger}_{\boldsymbol{k}2s} c_{\boldsymbol{k}1s} \right\}$$ inter-layer

$$\mathcal{H}_{soc} = \sum_{l=1,2,3} \alpha_l \sum_{\boldsymbol{k},s,s'} \boldsymbol{g}_{\boldsymbol{k}} \cdot \boldsymbol{\sigma}_{ss'} c^{\dagger}_{\boldsymbol{k}s} c_{\boldsymbol{k}s'}$$ Rashba-SOC

Superlattice – Ce115 / Yb115

paramagnetic limiting

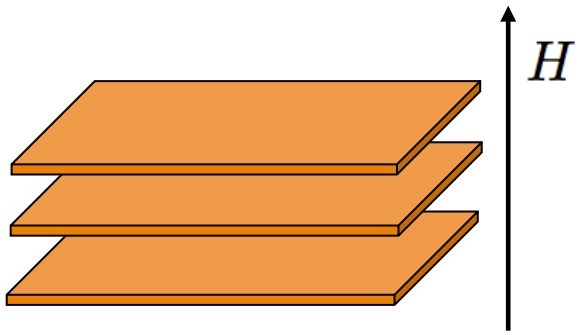

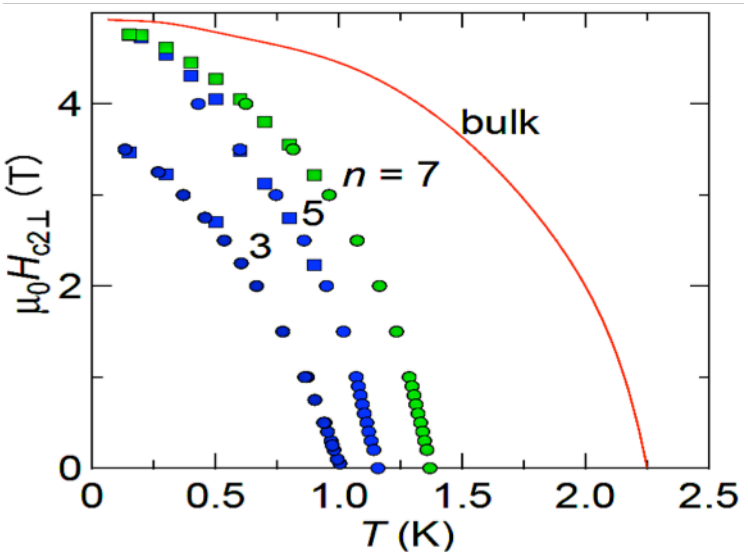

Matsuda group

Comparison with orbital depairing

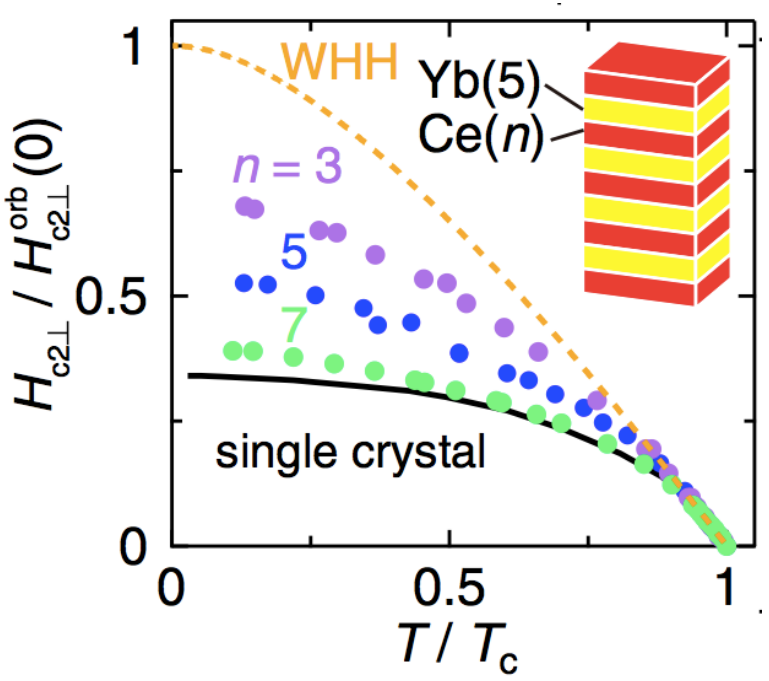

Rashba spin-orbit coupling
reduces the paramagnetic limit

due van Vleck spin polarization

smaller n ⇨ more boundary layers

⇨ more robust

Superlattice – Ce115 / Yb115

pair density wave

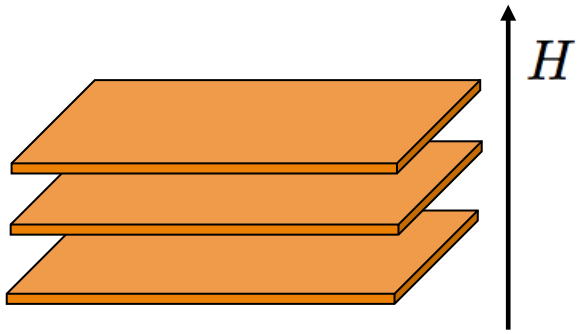

model system : without orbital depairing

Rashba SOC

$+\alpha$

0

$-\alpha$

BCS

$\hat{\Delta}^{(1)}$

$\hat{\Delta}^{(2)}$

$\hat{\Delta}^{(3)}$

PDW

$\hat{\Delta}^{(1)}$

0

$-\hat{\Delta}^{(3)}$

mixed-parity pairing

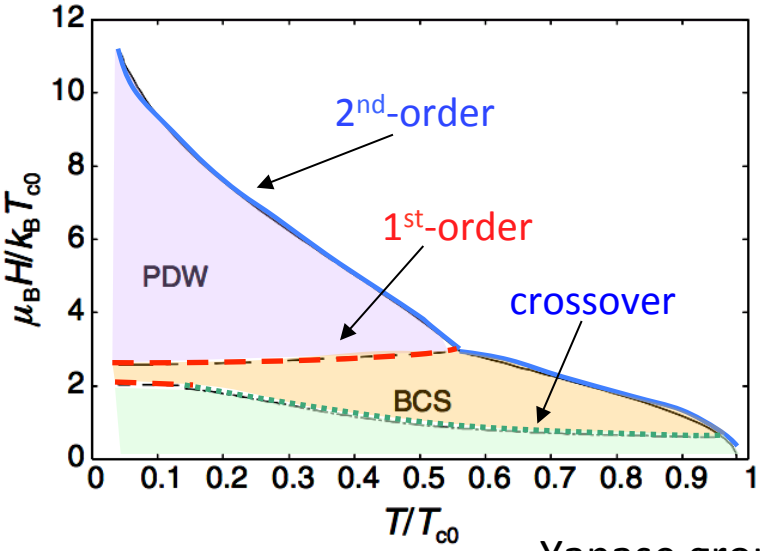

Yanase group

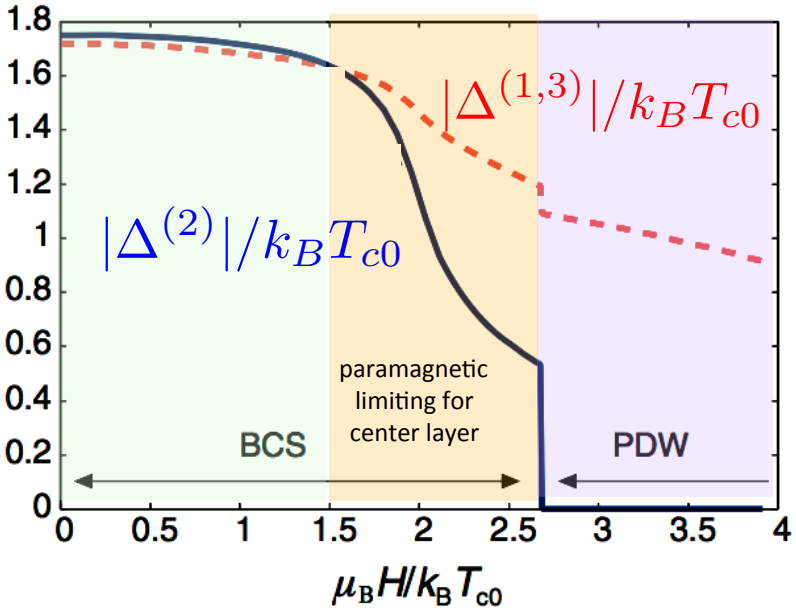

Helical phase - heterostructure

in-plane magnetic field

Edelstein; Dimitrova & Feigelman
Kaur, Agterberg & MS …

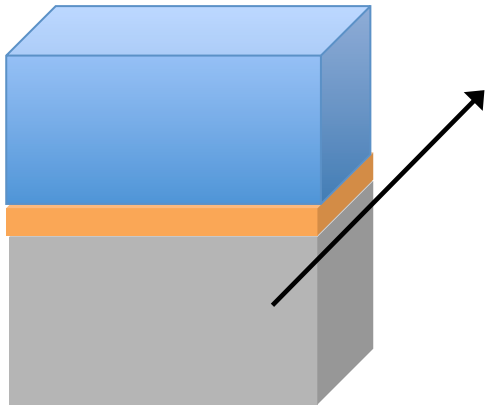

H_y

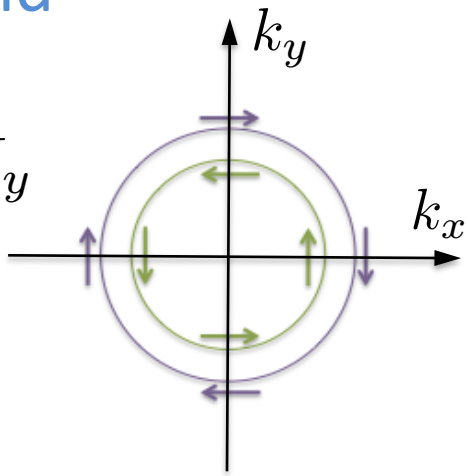

Δ

$\boldsymbol{q} \propto \hat{\boldsymbol{z}} \times \boldsymbol{H}$

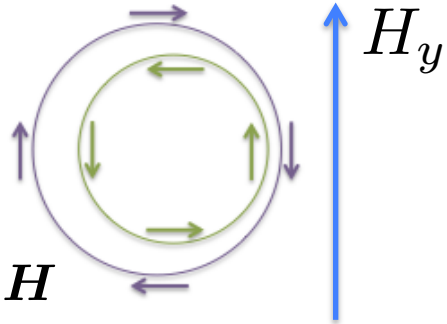

helical phase

$\Delta e^{i\boldsymbol{q}\cdot\boldsymbol{r}}$

FFLO-like state

Helical phase - heterostructure

in-plane magnetic field

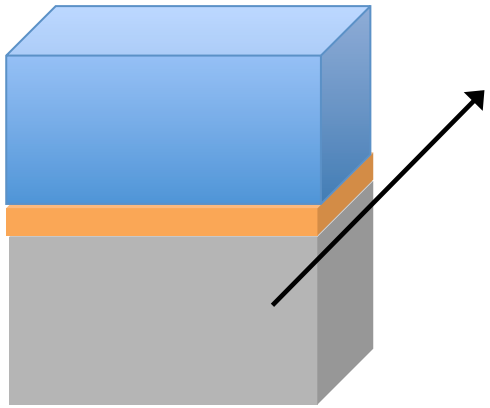

H_y

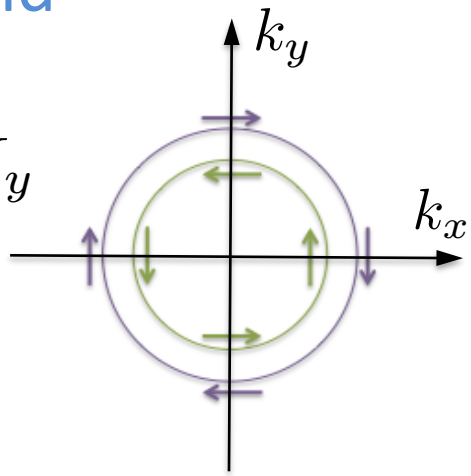

Δ

Edelstein; Dimitrova & Feigelman
Kaur, Agterberg & MS …

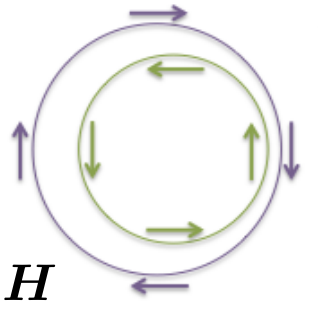

H_y

$\boldsymbol{q} \propto \hat{\boldsymbol{z}} \times \boldsymbol{H}$

helical phase

$\Delta e^{i\boldsymbol{q}\cdot\boldsymbol{r}}$

FFLO-like state

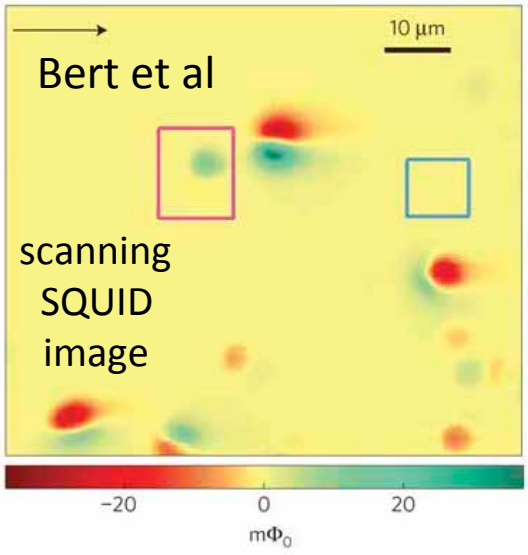

coexistence of SC and inplane ferromagnetism

Lu et al (Mannhart-Ashoori groups)
Bert et al (Hwang-Moler groups)

Michaeli, Potter & Lee: { coexistence of SC & FM in a helical phase (robustness)

Helical phase - heterostructure

in-plane magnetic field

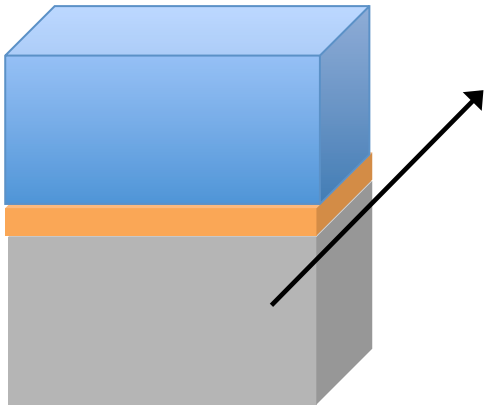

$$\Delta e^{i\boldsymbol{q}\cdot\boldsymbol{r}}$$

gauge freedom

$$\boldsymbol{q} = K(\hat{\boldsymbol{z}} \times \boldsymbol{H}) - \frac{2e}{\hbar c}\boldsymbol{A} = \boldsymbol{q}_0 - \frac{2e}{\hbar c}\boldsymbol{A}$$

Inhomogeneous phase

order parameter rigid

$$\boldsymbol{q} = const$$

$$\boldsymbol{B} = \frac{\hbar c}{2e}\boldsymbol{\nabla} \times \boldsymbol{q}_0 \perp \hat{\boldsymbol{z}}$$

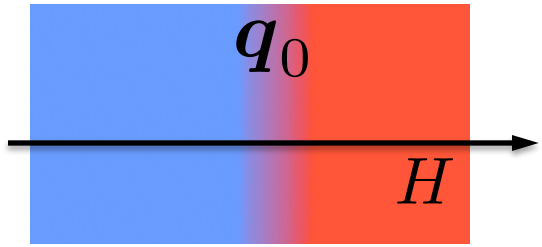

spatial variation in $\boldsymbol{q}_0$

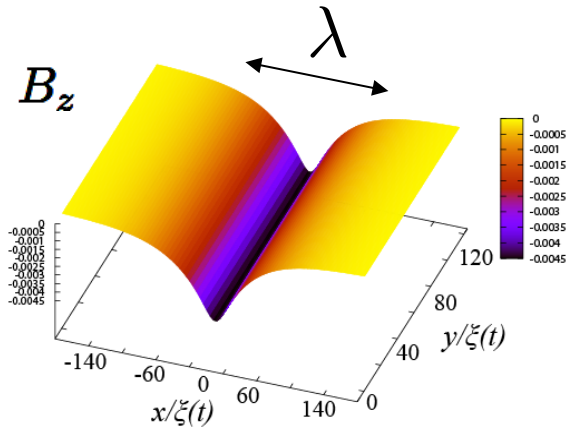

Aoyama & MS

Helical phase - superlattice – Ce115 / Yb115

in-plane magnetic field

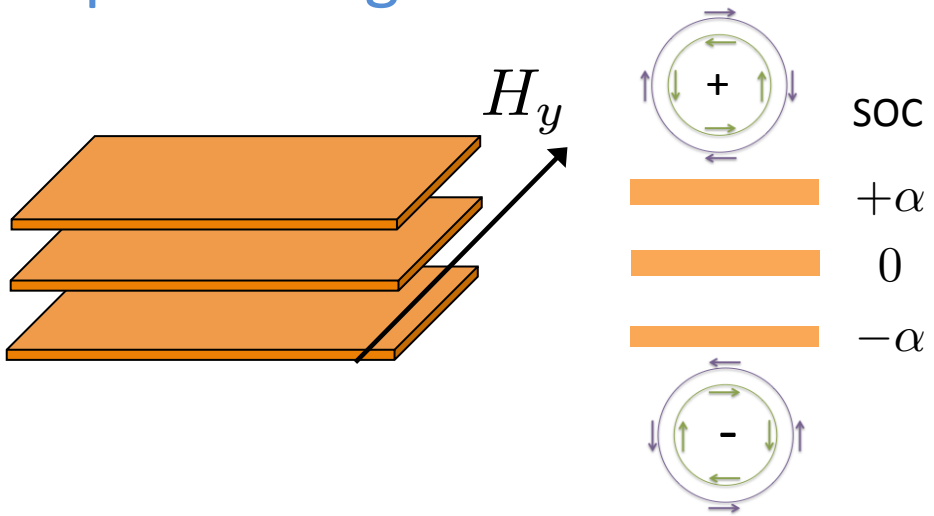

model - helical phase

pure helical phases

$$\hat{\Delta}_0^{(1)} e^{+iqx}$$

$$\hat{\Delta}_0^{(2)}$$

$$\hat{\Delta}_0^{(3)} e^{-iqx}$$

$$t_c = 0$$

Helical phase - superlattice – Ce115 / Yb115

in-plane magnetic field

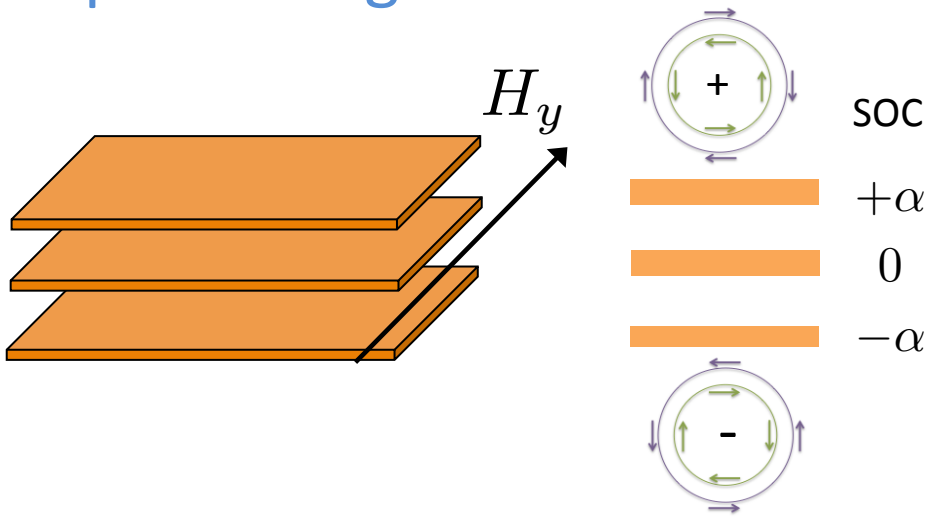

model - helical phase

pure helical phases	interlayer transfer
$\hat{\Delta}_0^{(1)} e^{+iqx}$	$\hat{\Delta}_0^{(1)} (e^{iqx} + \epsilon\, e^{-iqx})$
$\hat{\Delta}_0^{(2)}$	$\hat{\Delta}_0^{(2)} (e^{iqx} + e^{-iqx})$
$\hat{\Delta}_0^{(3)} e^{-iqx}$	$\hat{\Delta}_0^{(3)} (\epsilon\, e^{iqx} + e^{-iqx})$
$t_c = 0$	$t_c \neq 0$

Helical phase - superlattice – Ce115 / Yb115

in-plane magnetic field

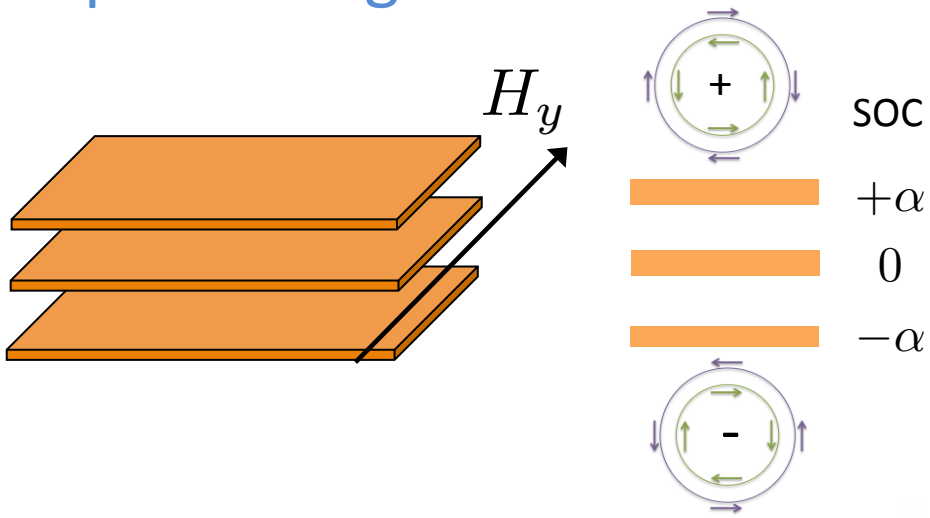

model - helical phase

pure helical phases

$$\hat{\Delta}_0^{(1)} e^{+iqx}$$
$$\hat{\Delta}_0^{(2)}$$
$$\hat{\Delta}_0^{(3)} e^{-iqx}$$

interlayer transfer

$$\hat{\Delta}_0^{(1)} (e^{iqx} + \epsilon\, e^{-iqx})$$
$$\hat{\Delta}_0^{(2)} (e^{iqx} + e^{-iqx})$$
$$\hat{\Delta}_0^{(3)} (\epsilon\, e^{iqx} + e^{-iqx})$$

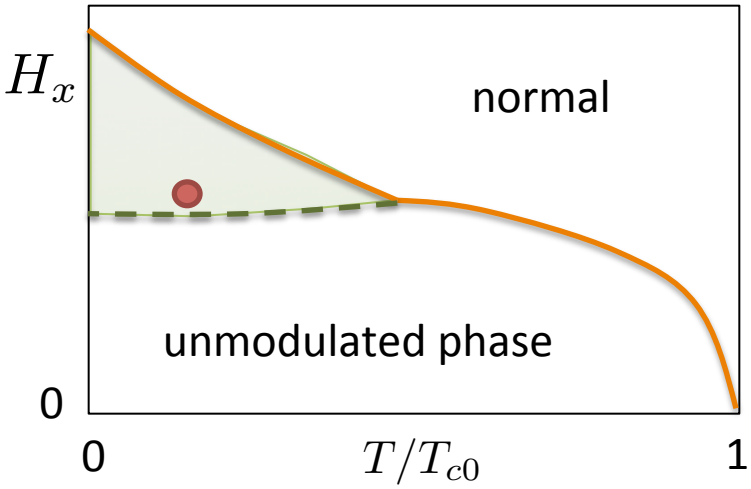

Larkin-Ovchinikov-like modulation

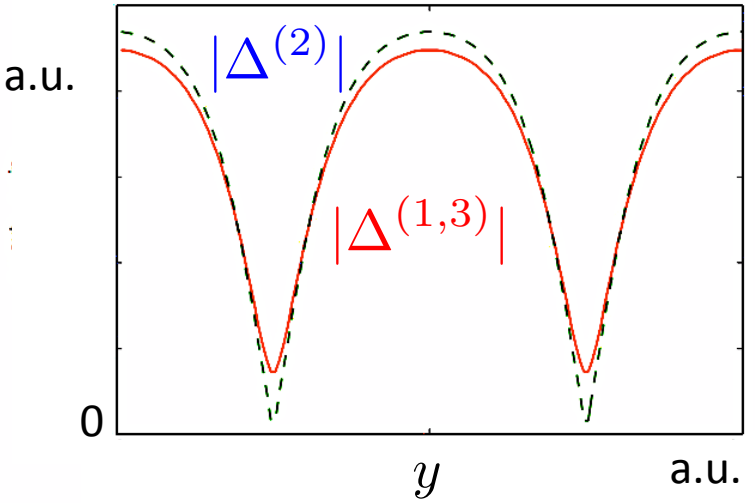

Helical phase - superlattice – Ce115 / Yb115

in-plane magnetic field

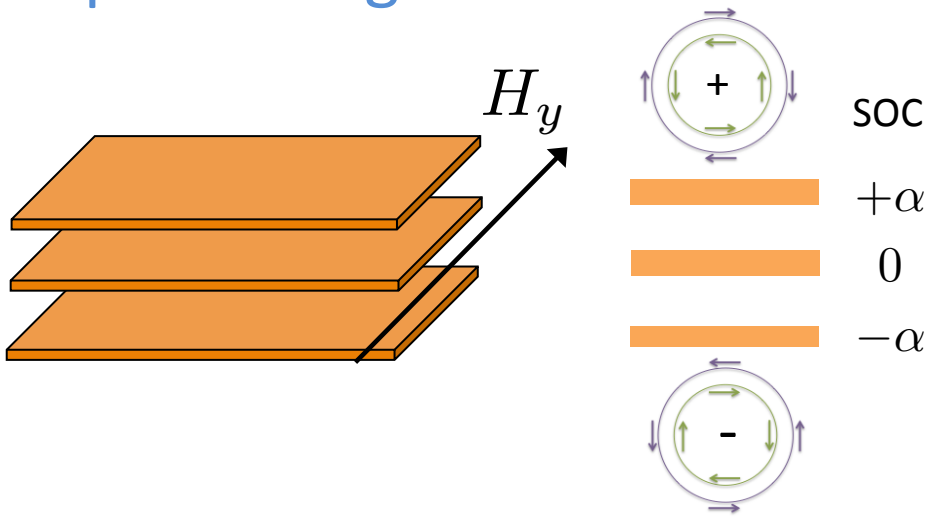

model - helical phase

pure helical phases

$$\hat{\Delta}_0^{(1)} e^{+iqx}$$
$$\hat{\Delta}_0^{(2)}$$
$$\hat{\Delta}_0^{(3)} e^{-iqx}$$

interlayer transfer

$$\hat{\Delta}_0^{(1)} (e^{iqx} + \epsilon\, e^{-iqx})$$
$$\hat{\Delta}_0^{(2)} (e^{iqx} + e^{-iqx})$$
$$\hat{\Delta}_0^{(3)} (\epsilon\, e^{iqx} + e^{-iqx})$$

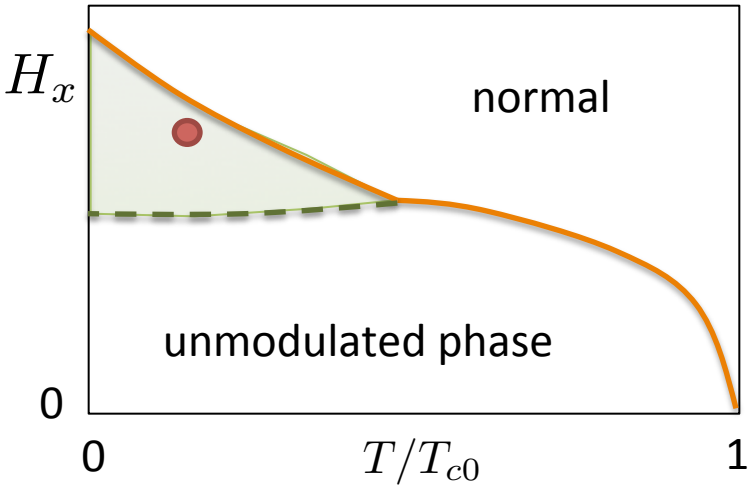

Fulde-Ferrel-like modulation

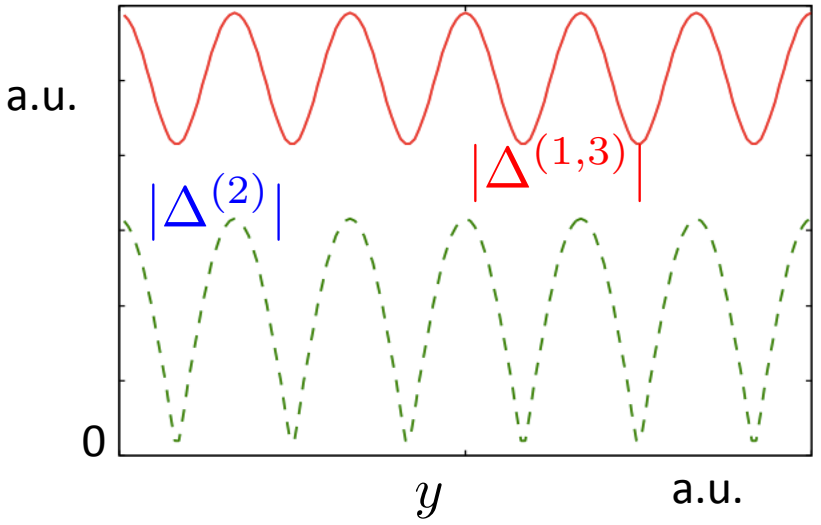

3-Kelvin phase
In
Ru-Sr_2RuO_4 eutectics

Sr_2RuO_4 - unconventional superconductor

Sr_2RuO_4

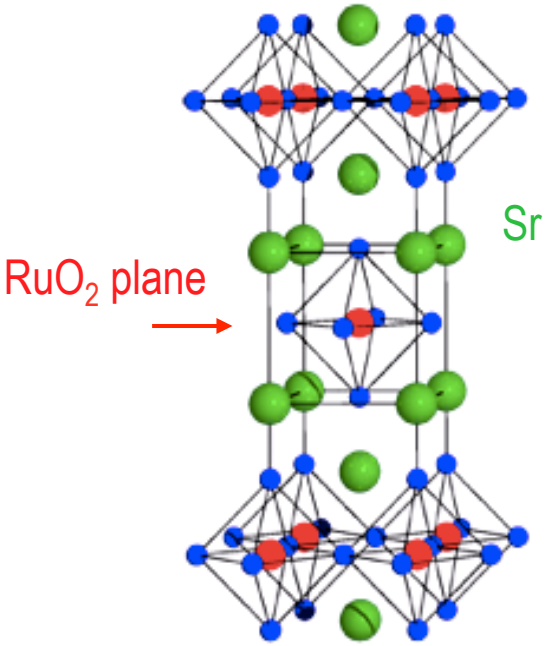

Maeno et al (1994)

$$T_c \approx 1.5\mathrm{K}$$

pairing symmetry

spin-triplet odd-parity

$$\vec{d}(\vec{k}) = \hat{z}\ (k_x \pm ik_y)$$

chiral p-wave

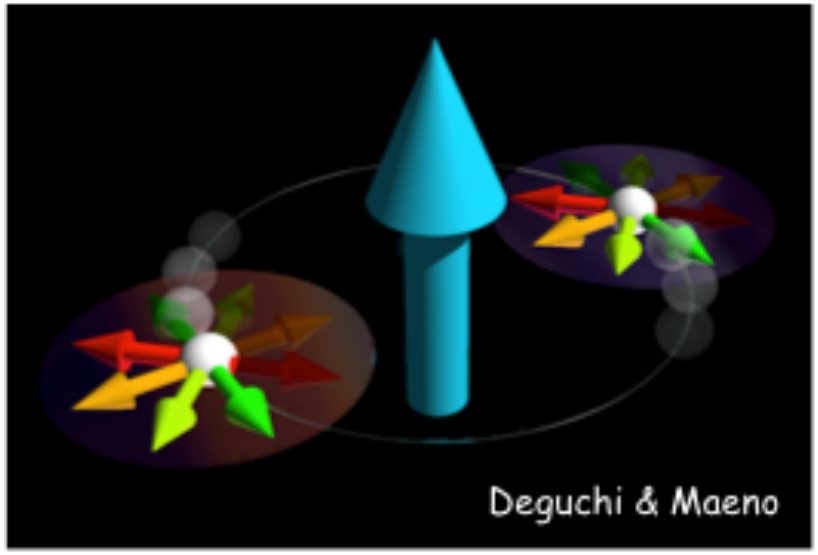

Eutectic Sr_2RuO_4-Ru

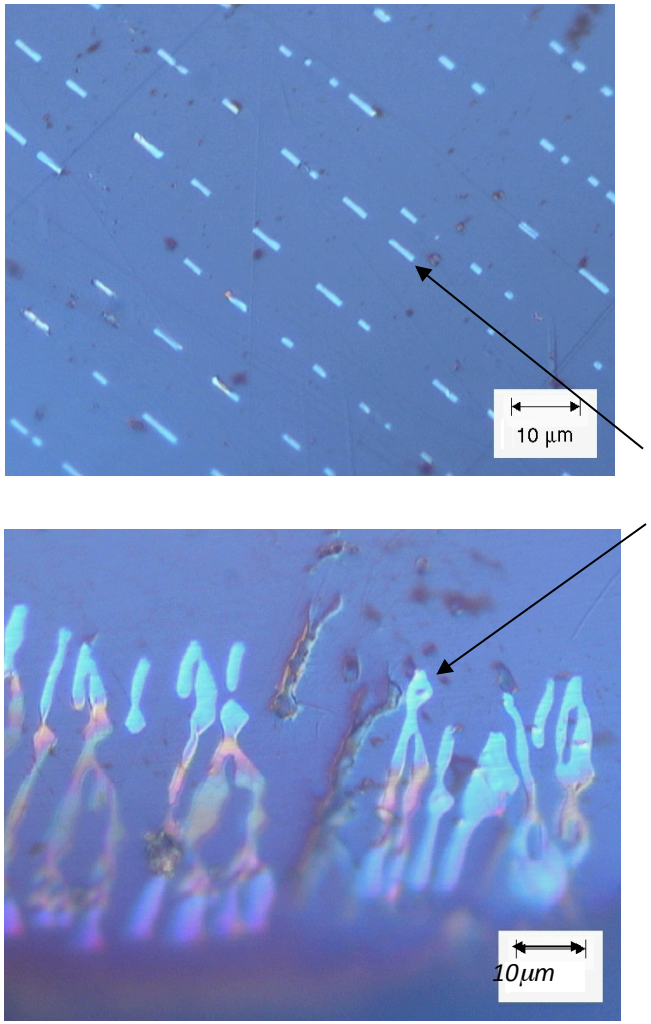

µm-sized Ru-metal inclusions

Maeno et al (1997)

nucleation of inhomogeneous superconductivity

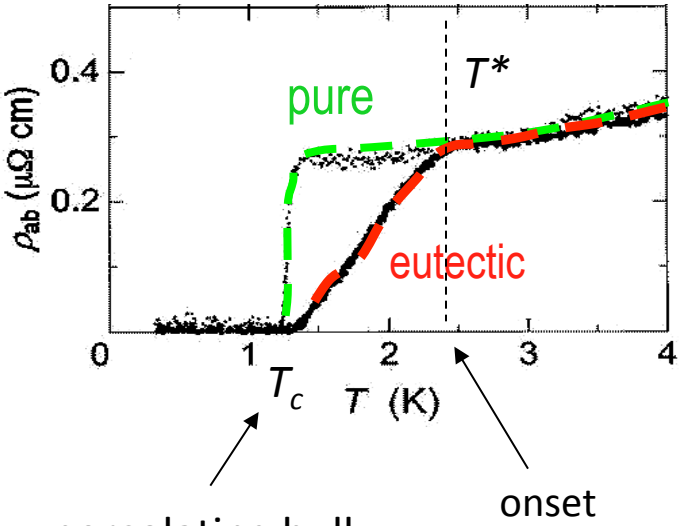

$T^* \sim 2xT_c \sim 3\ K$

"3 - Kelvin phase"

Eutectic Sr_2RuO_4-Ru - nucleation

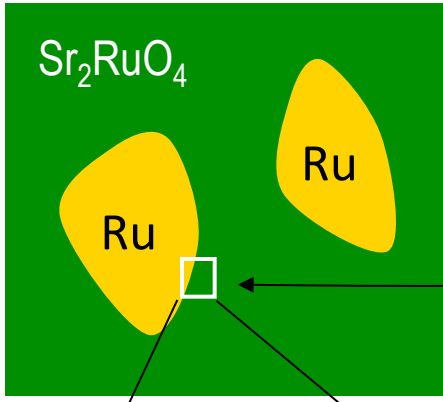

superconductivity nucleates at interface

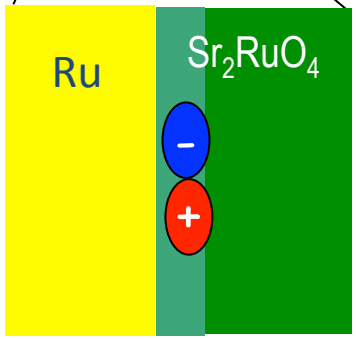

MS & Monien

energetically favored
time reversal symmetry
conserving

Eutectic Sr_2RuO_4-Ru - nucleation

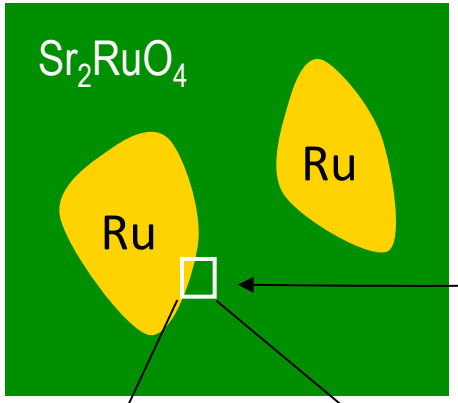

superconductivity nucleates at interface

very clean interfaces

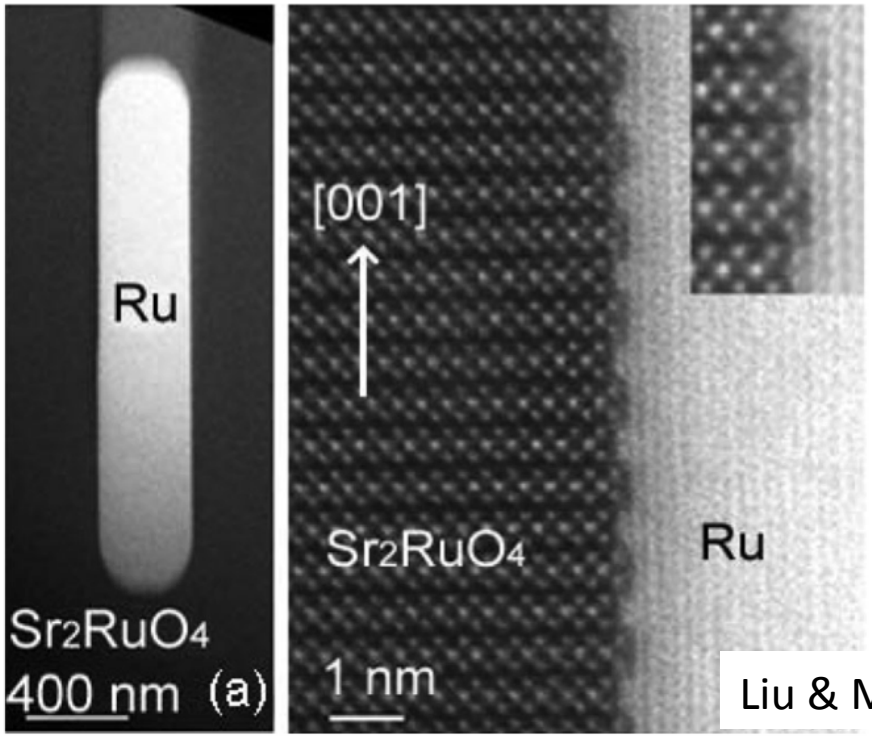

Liu & Mao groups

MS & Monien

energetically favored
time reversal symmetry
conserving

Eutectic Sr_2RuO_4-Ru - nucleation

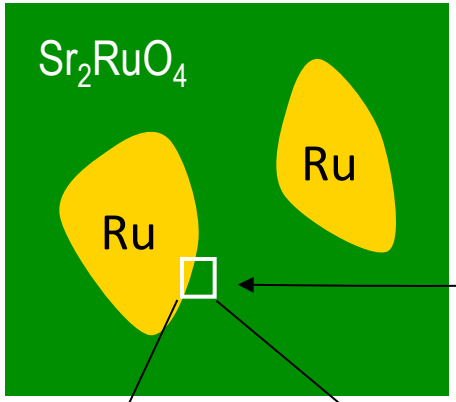

superconductivity nucleates at interface

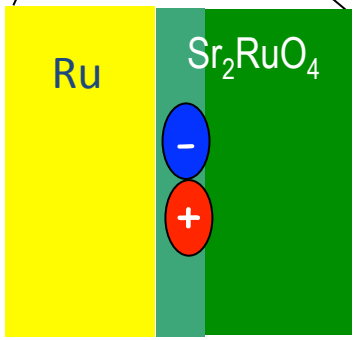

~ 20 nm

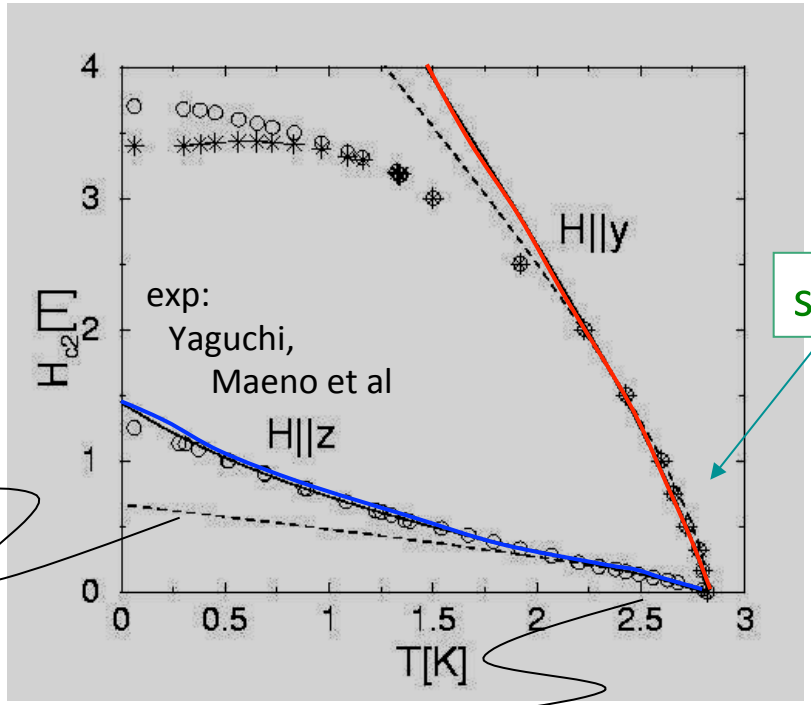

sublinear

filamentary superconductivity

theo: Belardinelli, Matsumoto & MS

Sequence of phases

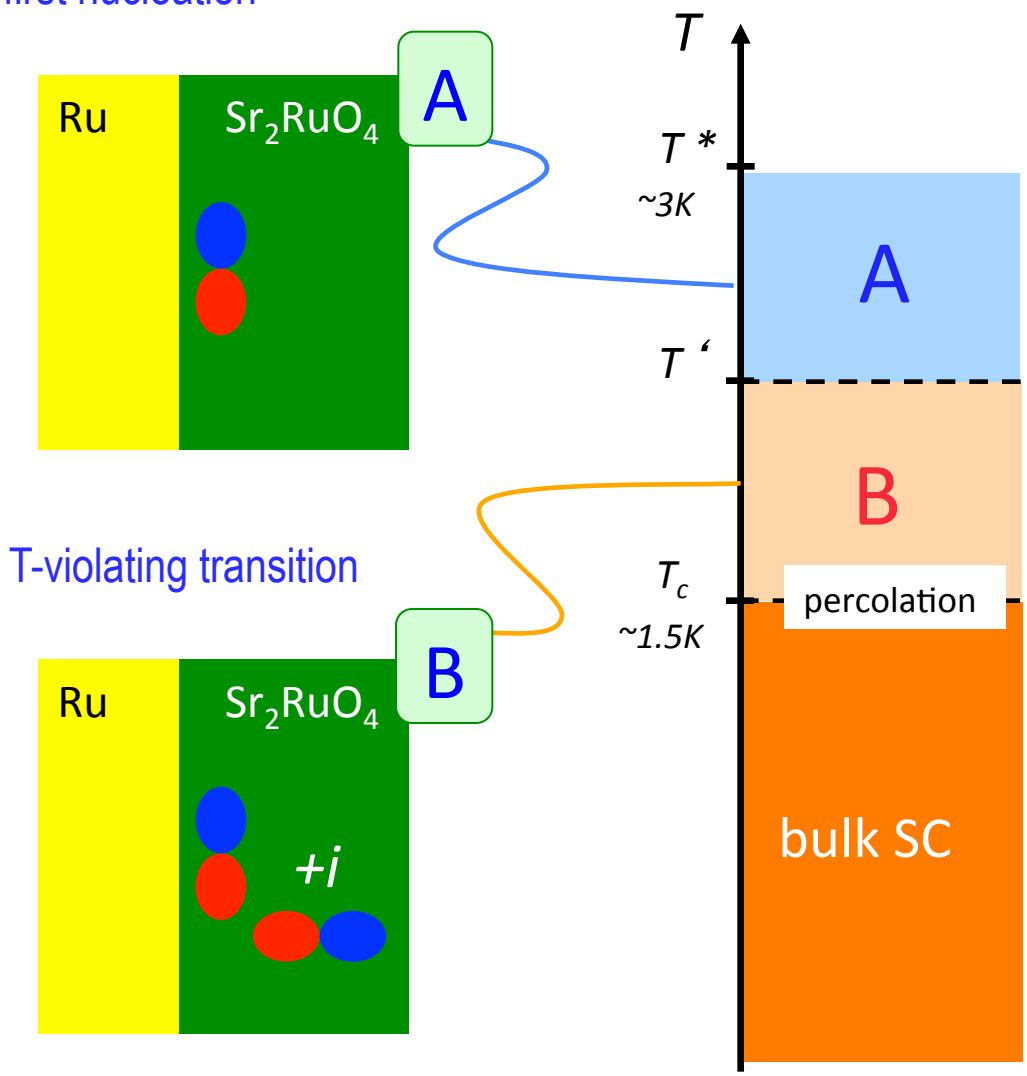

Kaneyasu et al (2010)

Sequence of phases

first nucleation

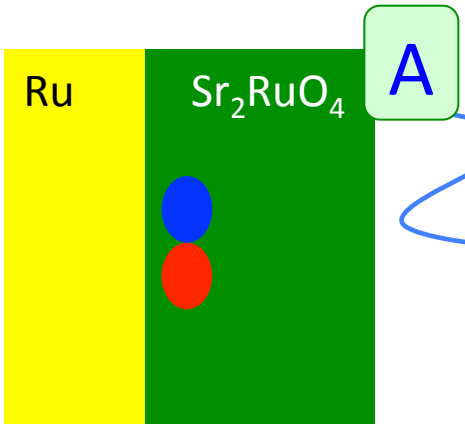

T-violating transition

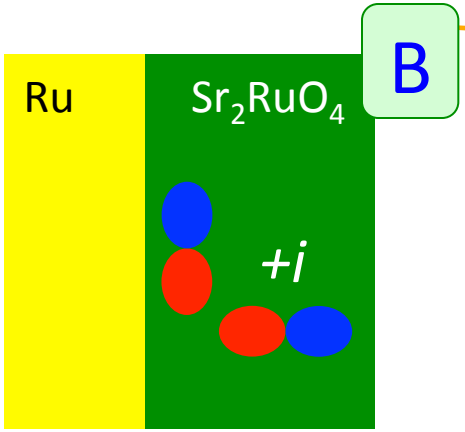

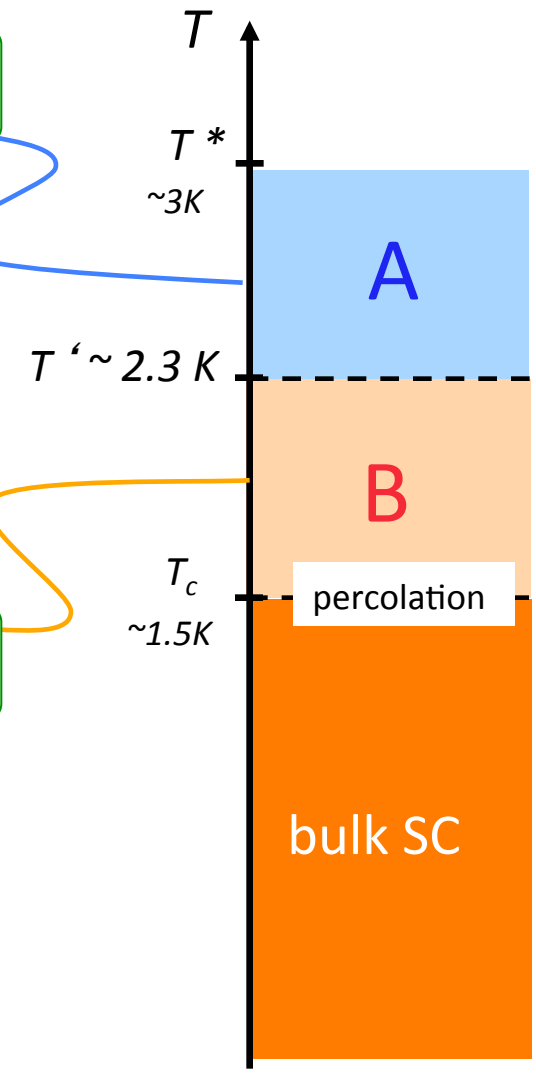

Kaneyasu et al (2010)

critical current of 3K-phase

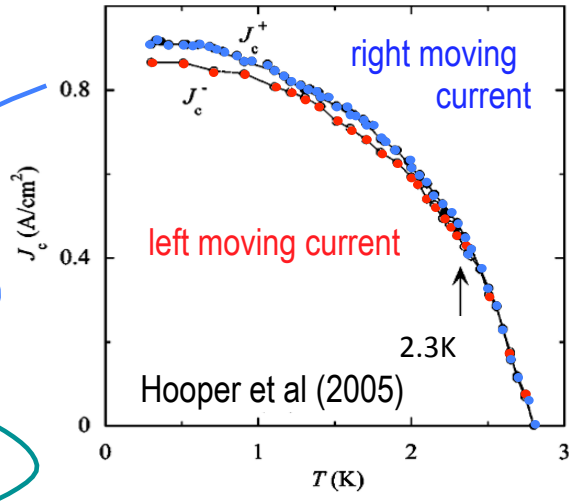

tunneling Ru-Sr_2RuO_4

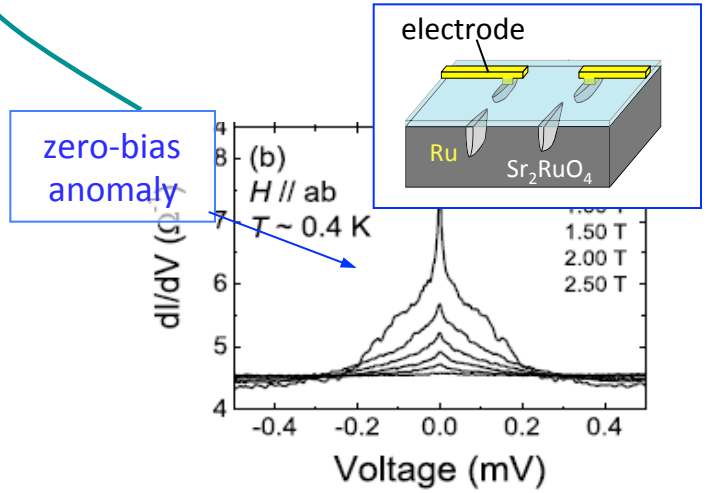

Yaguchi et al (2006)

A-to-B transition - zero-bias anomaly

Tunneling through Ru-inclusions

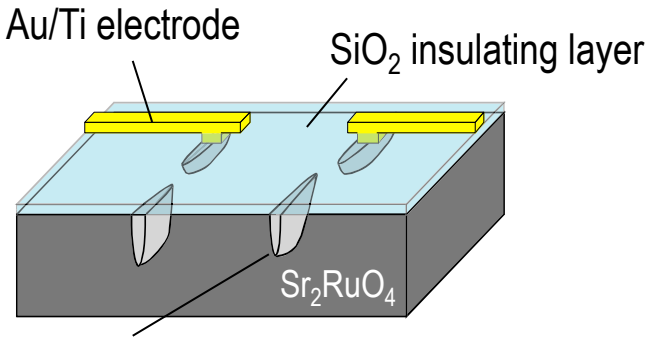

Kawamura et al.

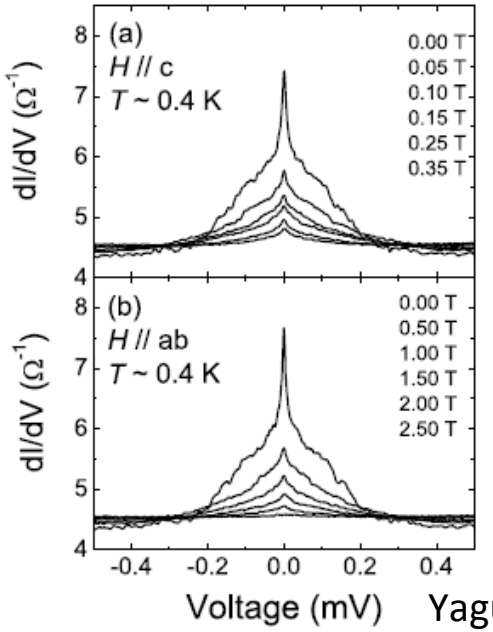

Yaguchi, Maeno et al.

A-to-B transition - zero-bias anomaly

Tunneling through Ru-inclusions

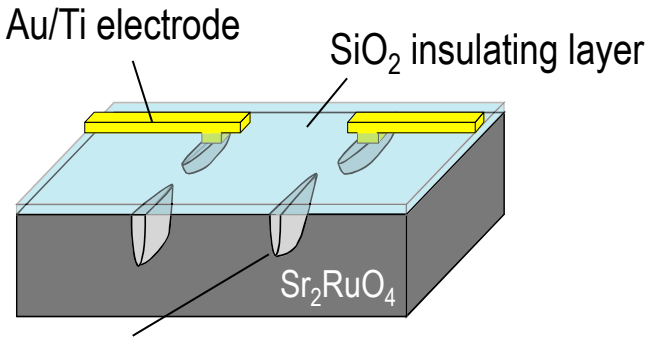

Kawamura et al.

onset of
zero-bias anomaly at

$$T' \approx 2.3\mathrm{K}$$

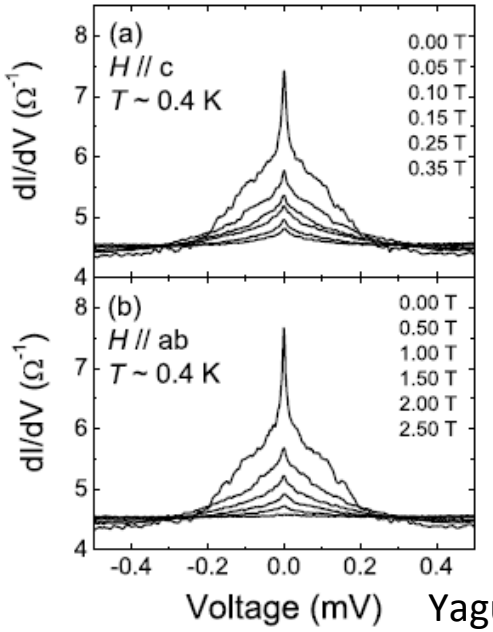

Yaguchi, Maeno et al.

A-to-B transition - zero-bias anomaly

Tunneling spectroscopy

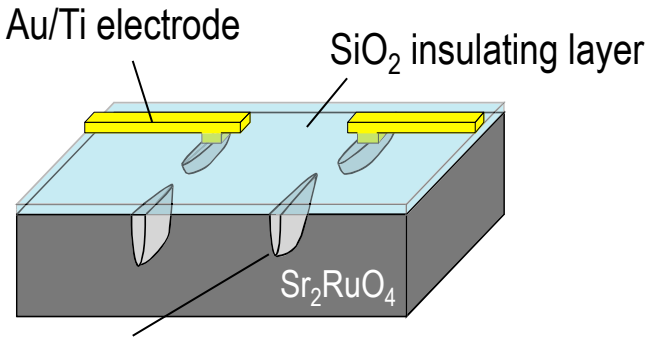

Kawamura et al.

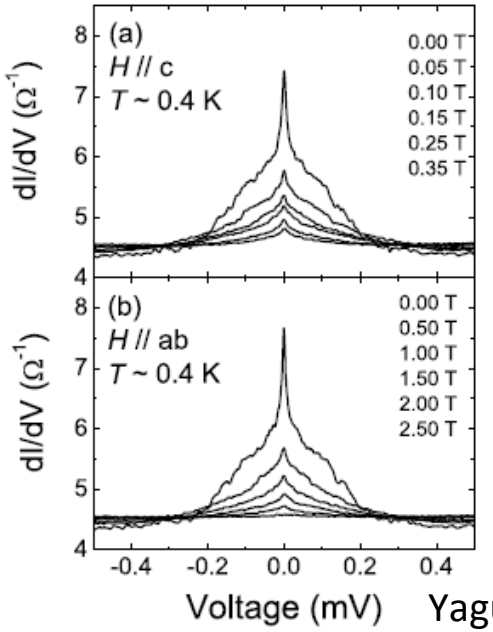

Yaguchi, Maeno et al.

Andreev bound states

parallel component

A

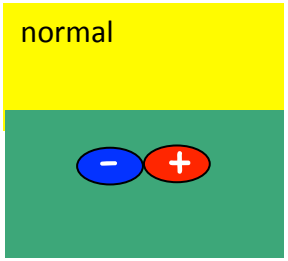

no bound states

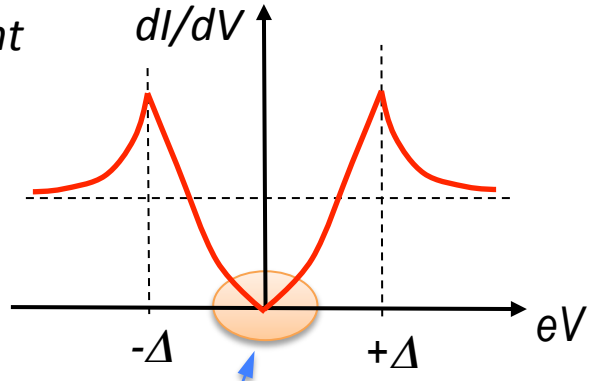

line node in gap

chiral combination

B

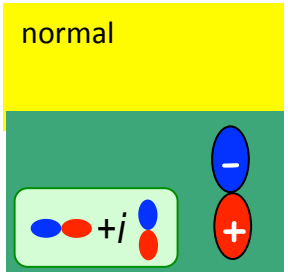

chiral edge states

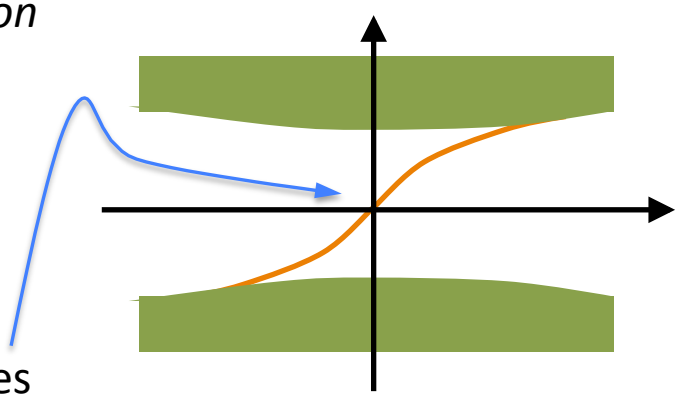

A-to-B transition - zero-bias anomaly

Tunneling spectroscopy

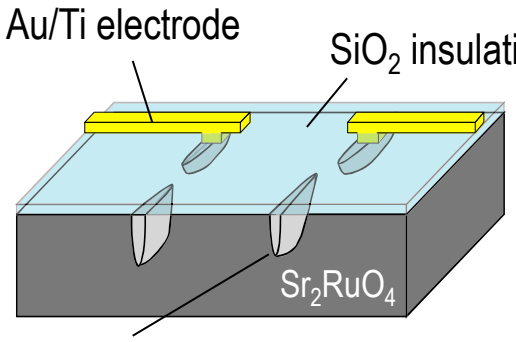

Kawamura et al.

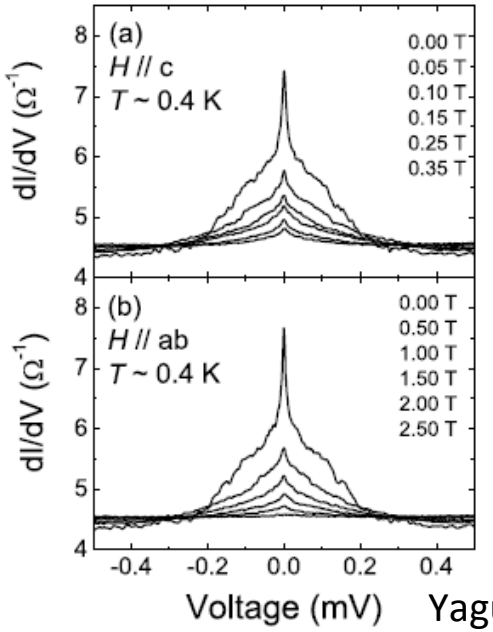

Yaguchi, Maeno et al.

Andreev bound states

parallel component

A

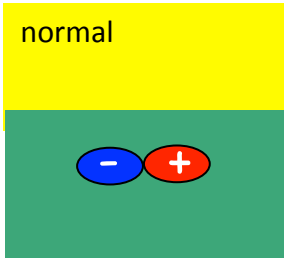

no bound states

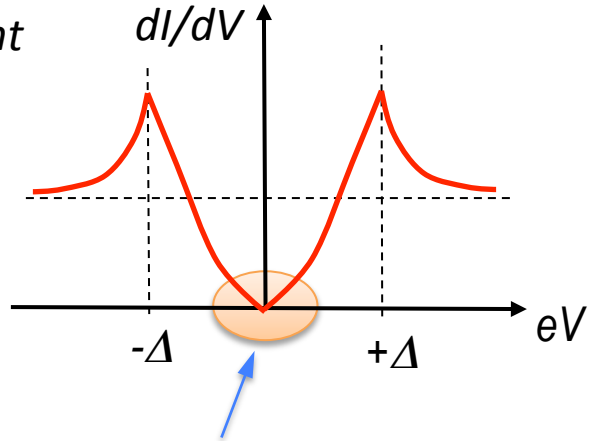

line node in gap

chiral combination

B

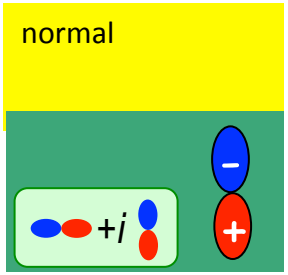

chiral edge states

zero-bias anomaly

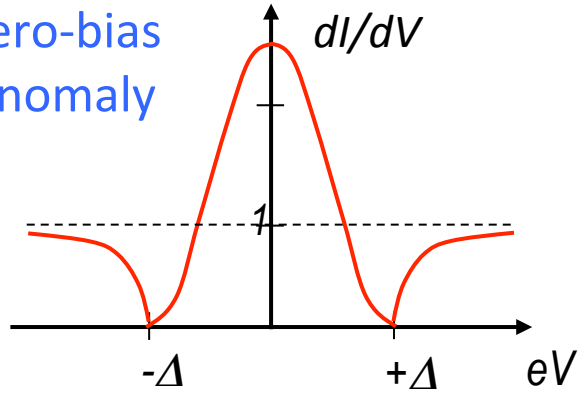

A-to-B transition - zero-bias anomaly

magnetic field

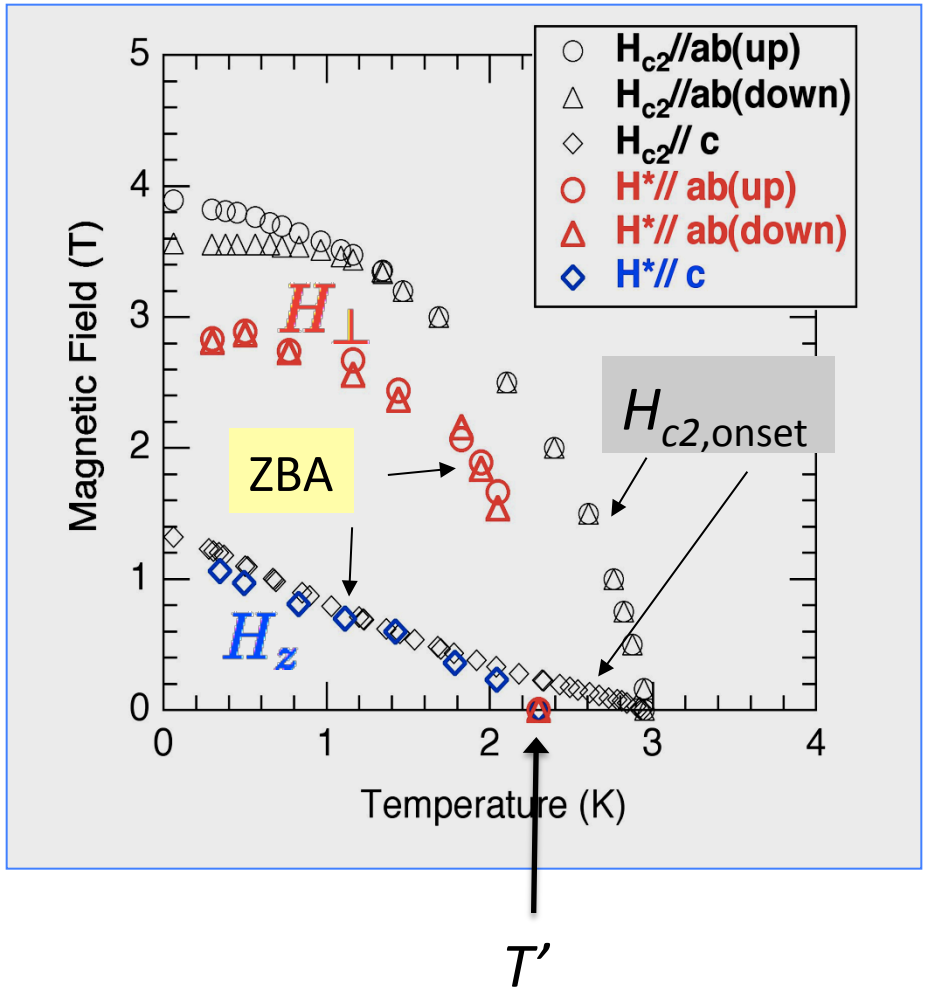

direct contacts to Ru-inclusions

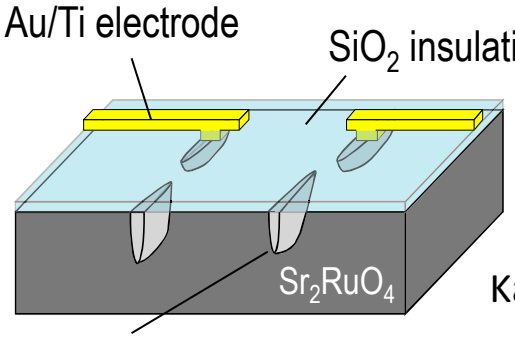

Kawamura et al.

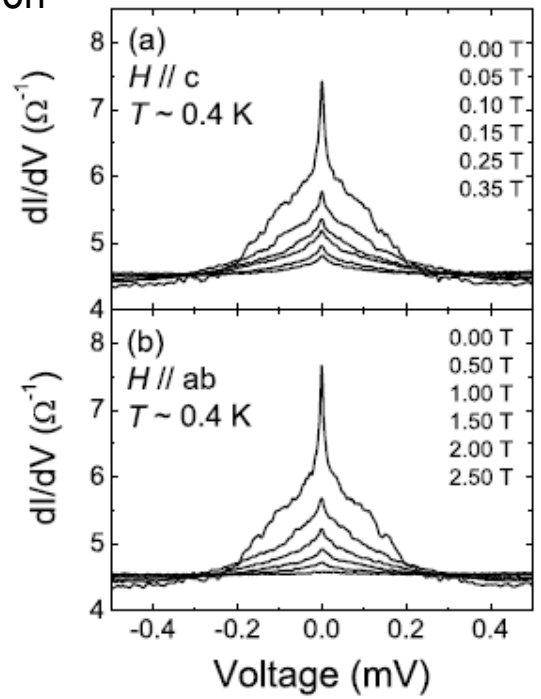

A-to-B transition - zero-bias anomaly

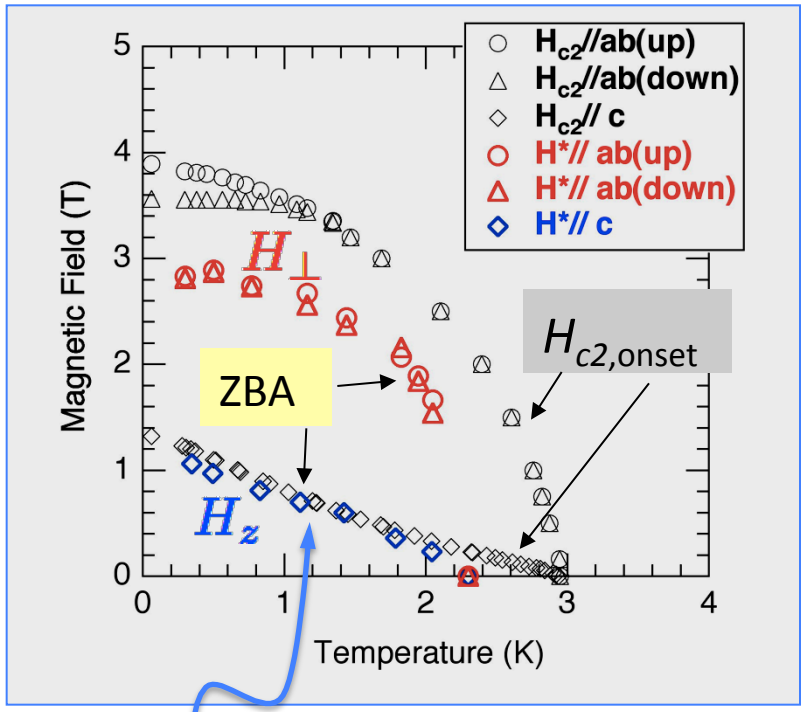

magnetic field induces perpendicular component once parallel component is present

parallel component

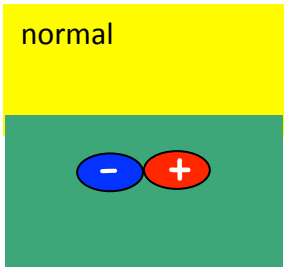

perpendicular component

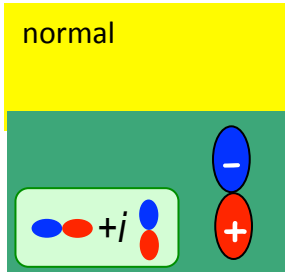

magnetic field parallel *z*-axis

Zeeman coupling to

Cooper pair angular momentum

$$L_z \propto i(\eta_x^*\eta_y - \eta_x\eta_y^*)$$

$$F_Z = i\gamma H_z(\eta_x^*\eta_y - \eta_x\eta_y^*)$$

Anomalous Josephson coupling

device – Josephson coupling

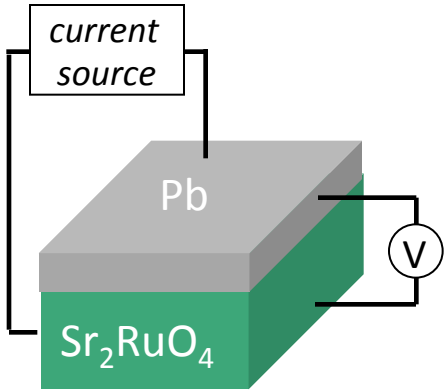

Nakamura, Maeno et al (2010)

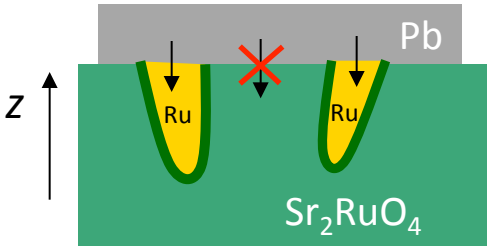

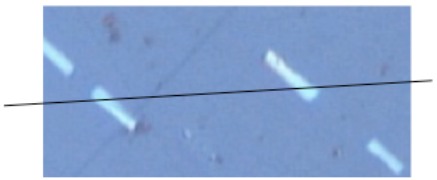

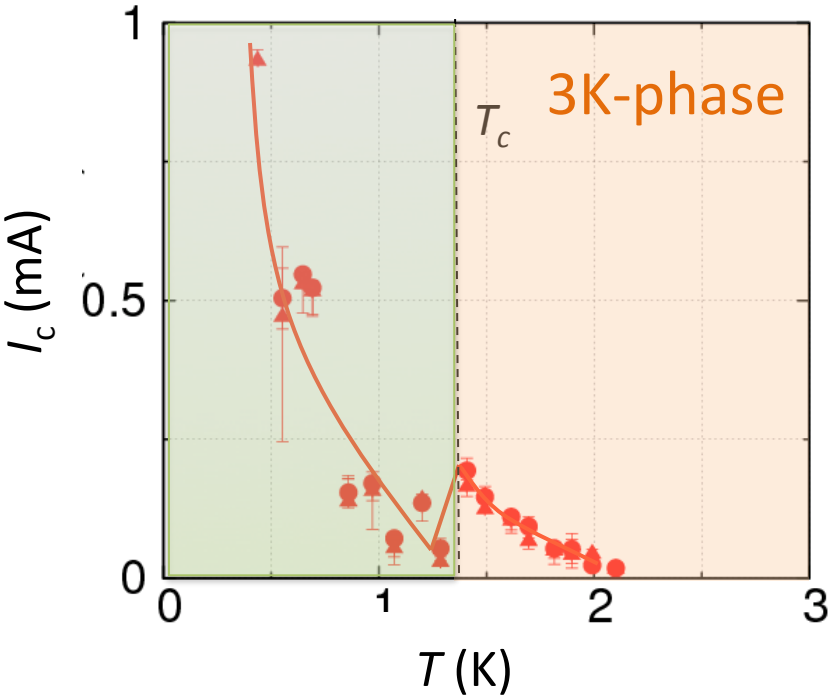

Anomalous Josephson coupling

device – Josephson coupling

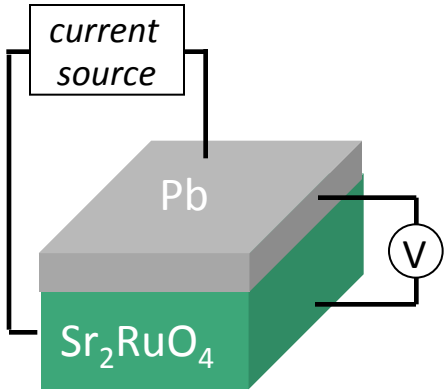

Nakamura, Maeno et al (2010)

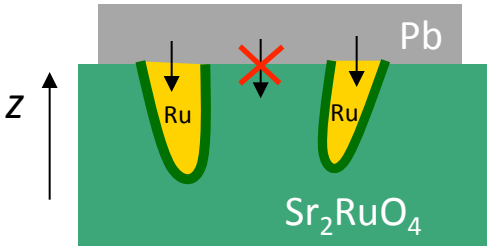

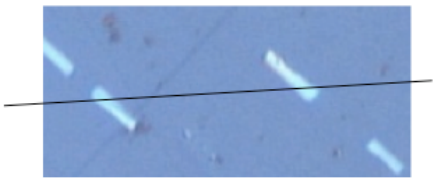

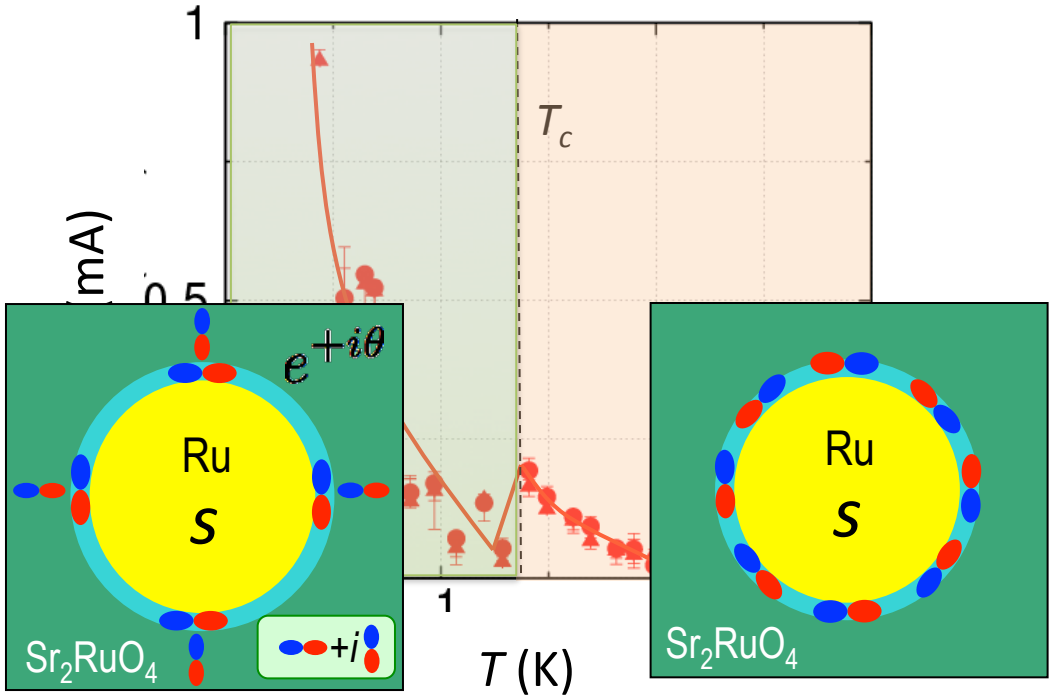

frustrated coupling into chiral p-wave

Etter et al

coupling through Ru to 3K-phase

Owen-Scalapino

Loops & half-flux quanta In Sr_2RuO_4

Half-flux quantization

Sr_2RuO_4 micro-loops

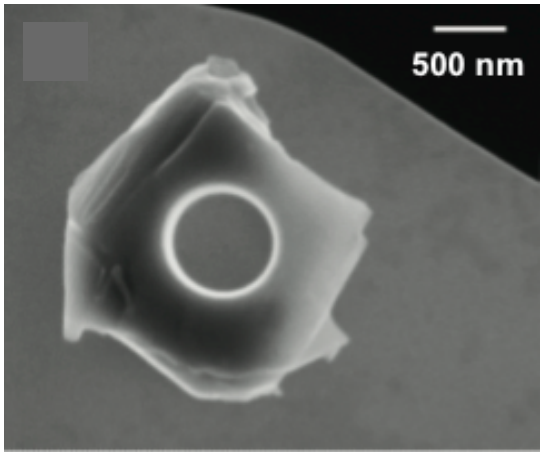

cantilever magnetometer

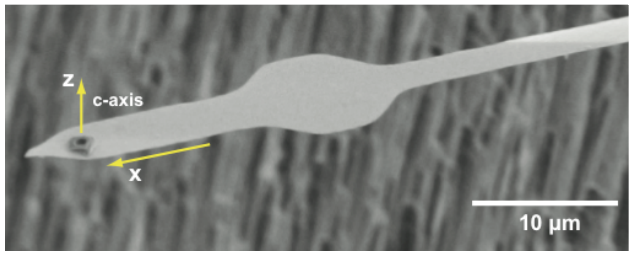

Budakian et al

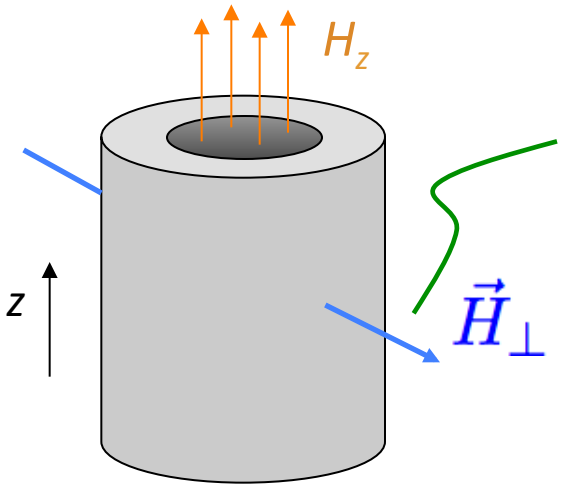

inplane field supports

half-flux quantum steps

intermediate half-flux quantum

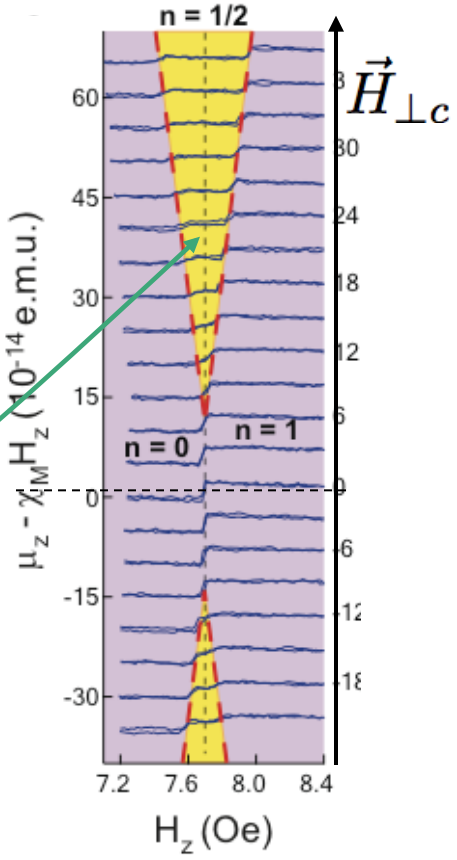

Jang et al (2010)

$$\Phi = \Phi_0/2$$

d-vector „manipulation“

d-texture / *d*-soliton

$$\boldsymbol{d}(\boldsymbol{k}) = \Delta \hat{\boldsymbol{d}} g(\boldsymbol{k})$$

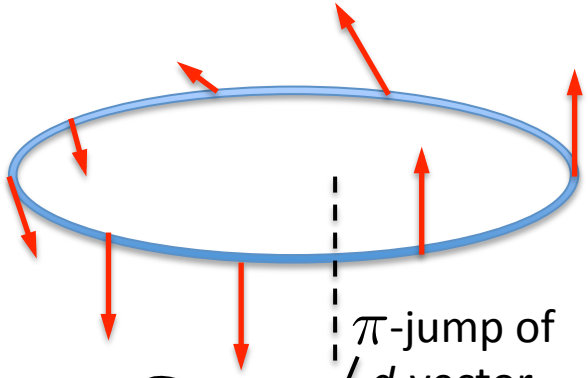

$$\boldsymbol{d}(\boldsymbol{k}, \boldsymbol{r}) = |\Delta(\boldsymbol{r})| e^{i\phi(\boldsymbol{r})} \hat{\boldsymbol{d}}(\boldsymbol{r}) g(\boldsymbol{k})$$

π-phase winding of ϕ

$$\Phi = \frac{\Phi_0}{2\pi} \int d\vec{l} \cdot \vec{\nabla}\phi = \frac{\Phi_0}{2}$$

half-flux quantum

Volovik & Salomaa ;Ivanov
Chung, Blum & Kim; .....

Vakaryuk & Leggett
Roberts, Budakian & Stone
Kee & MS

d-vector „manipulation“

d-texture / *d*-soliton

$$\boldsymbol{d}(\boldsymbol{k}) = \Delta \hat{\boldsymbol{d}} g(\boldsymbol{k})$$

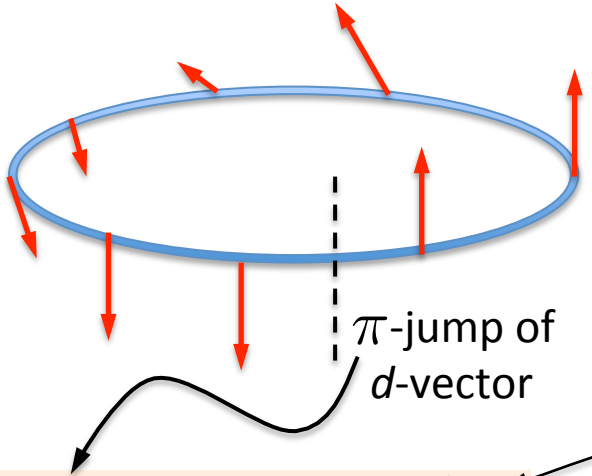

$$\boldsymbol{d}(\boldsymbol{k},\boldsymbol{r}) = |\Delta(\boldsymbol{r})| e^{i\phi(\boldsymbol{r})} \hat{\boldsymbol{d}}(\boldsymbol{r}) g(\boldsymbol{k})$$

π-phase winding of ϕ

$$\Phi = \frac{\Phi_0}{2\pi} \int d\vec{l} \cdot \vec{\nabla}\phi = \frac{\Phi_0}{2}$$

half-flux quantum

Volovik & Salomaa ;Ivanc
Chung, Blum & Kim; .....

Vakaryuk & Leggett
Roberts, Budakian & Sto
Kee & MS

weak
spin-orbit coupling

d-texture

strong
spin-orbit coupling

d-soliton

d-vector „manipulation“

d-texture / *d*-soliton

$$\boldsymbol{d}(\boldsymbol{k}) = \Delta \hat{\boldsymbol{d}} g(\boldsymbol{k})$$

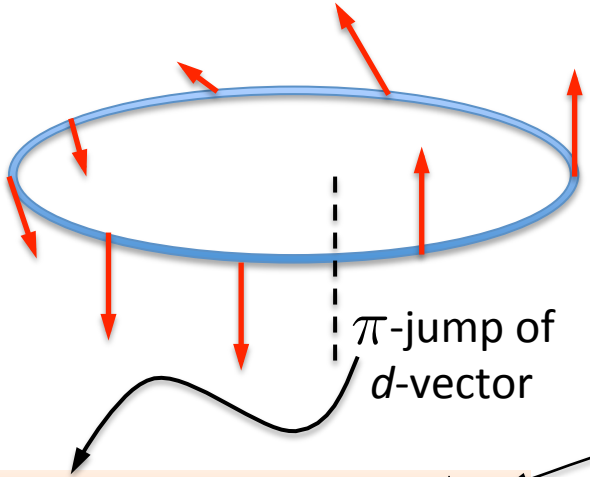

$$\boldsymbol{d}(\boldsymbol{k}, \boldsymbol{r}) = |\Delta(\boldsymbol{r})| e^{i\phi(\boldsymbol{r})} \hat{\boldsymbol{d}}(\boldsymbol{r}) g(\boldsymbol{k})$$

π-phase winding of ϕ

supercurrent:

$$J_\alpha \propto |\Delta|^2 \left(\boldsymbol{\nabla}\phi - \frac{2\pi}{\Phi_0} \boldsymbol{A} \right)_\alpha$$

spin current:

$$J_{\alpha m} \propto |\Delta|^2 \left(\hat{\boldsymbol{d}}^* \times \nabla_\alpha \hat{\boldsymbol{d}} \right)_m$$

spin polarization

$$S_m \propto \sum_\alpha J_\alpha J_{\alpha m}$$

d-vector „manipulation“

d-texture / *d*-soliton

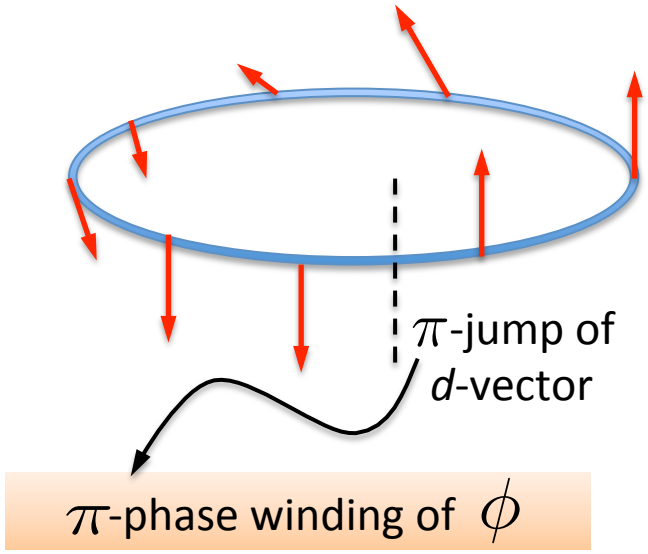

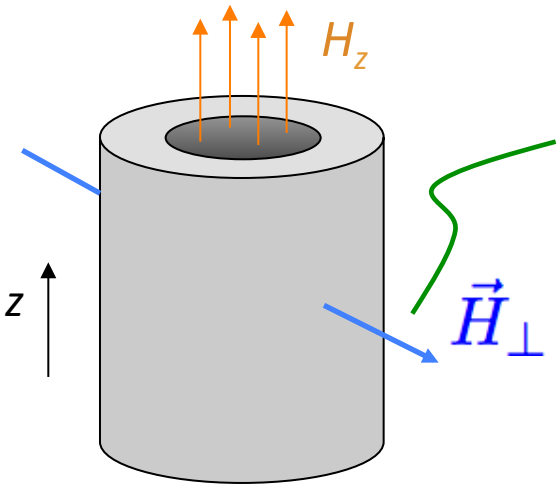

Budakian et al

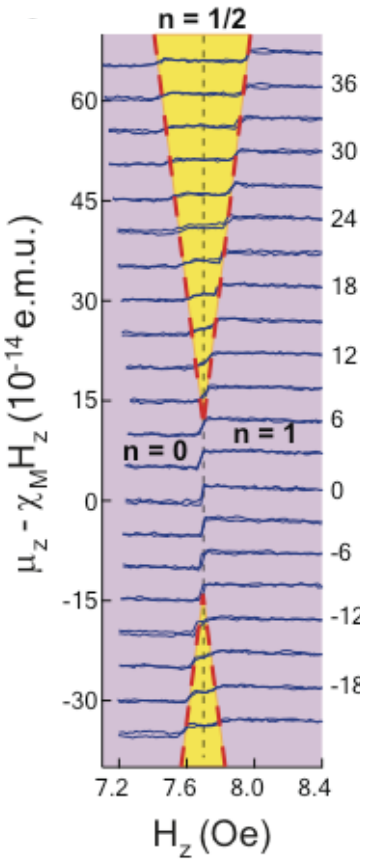

spin polarization

$$S_m \propto \sum_\alpha J_\alpha J_{\alpha m}$$

magnetic field perpendicular to *d*-twist facilitates *d*-texture / *d*-soliton

d-vector „manipulation“

d-twist in Josephson junctions

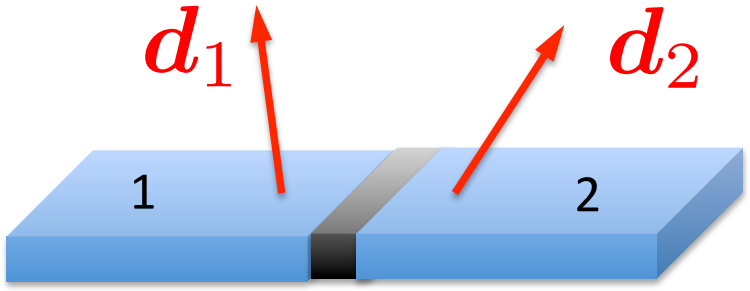

$\phi = \phi_2 - \phi_1$ Josephson phase

$\hat{\boldsymbol{d}}_1 \cdot \hat{\boldsymbol{d}}_2 = \cos\alpha$

Asano; Brydon, Manske et al, ….

Josephson current:

$$J = J_0 \cos\alpha \sin\phi$$

Josephson spin current:

$$J_s = J_{s0} \sin\alpha \cos\phi$$

d-vector „manipulation“

d-twist in Josephson junctions

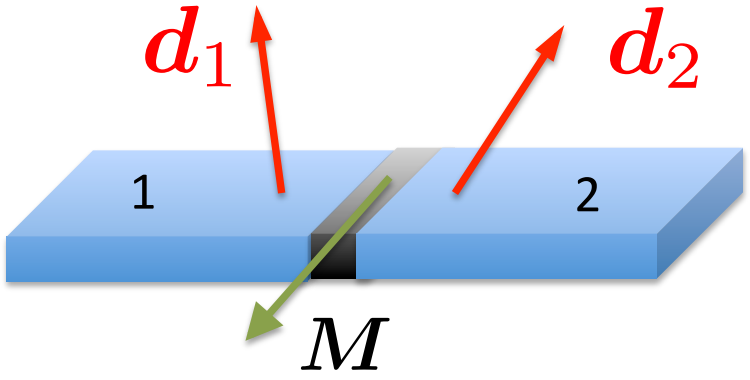

$\phi = \phi_2 - \phi_1$ Josephson phase

$\hat{\boldsymbol{d}}_1 \cdot \hat{\boldsymbol{d}}_2 = \cos\alpha$

Josephson current:

$$J = J_0 \cos\alpha \sin\phi$$

Josephson spin current:

$$J_s = J_{s0} \sin\alpha \cos\phi$$

junction magnetization modifies current-phase coupling

$$F_J = t\hat{\boldsymbol{d}}_1 \cdot \hat{\boldsymbol{d}}_2 \cos\phi + t'\boldsymbol{M} \cdot (\hat{\boldsymbol{d}}_1 \times \hat{\boldsymbol{d}}_2) \sin\phi$$

d-vector „manipulation“

d-twist in Josephson junctions

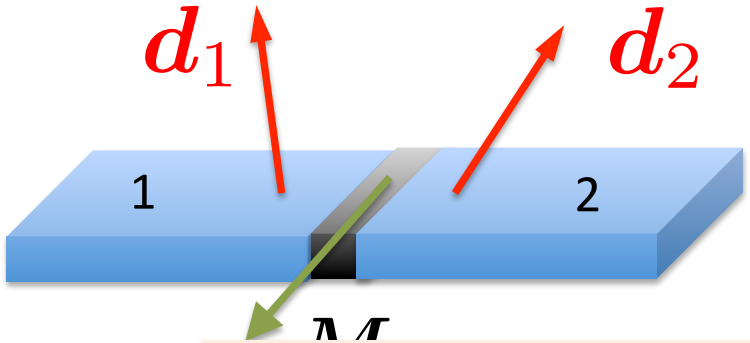

$\phi = \phi_2 - \phi_1$ Josephson phase

$\hat{\boldsymbol{d}}_1 \cdot \hat{\boldsymbol{d}}_2 = \cos\alpha$

Josepl

$J =$

junctio

ϕ

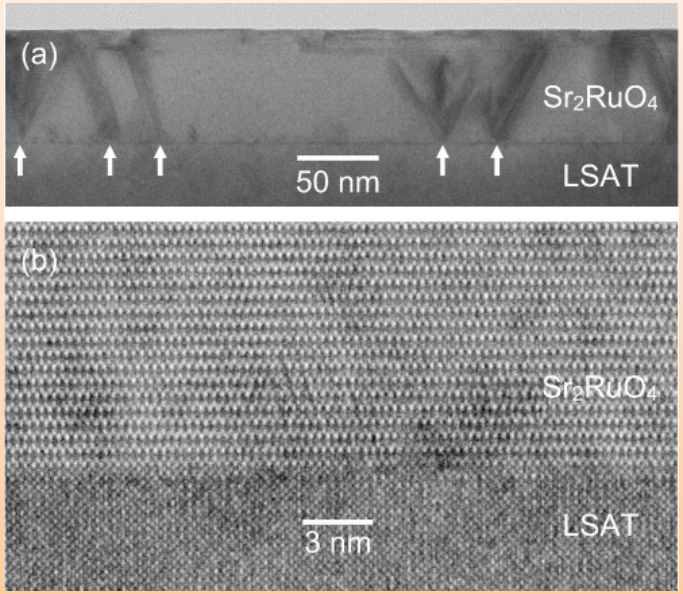

thin films of Sr_2RuO_4

Krockenberger et al (NTT)

$T_c \lesssim 1\mathrm{K}$

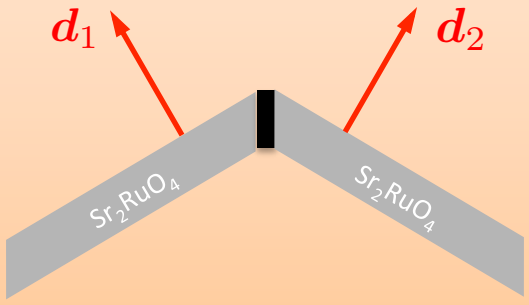

Opportunities – this is just the beginning

Structured samples

SmFeAs(O,F)

Focussed Ion Beam

Criticial current
in magnetic field

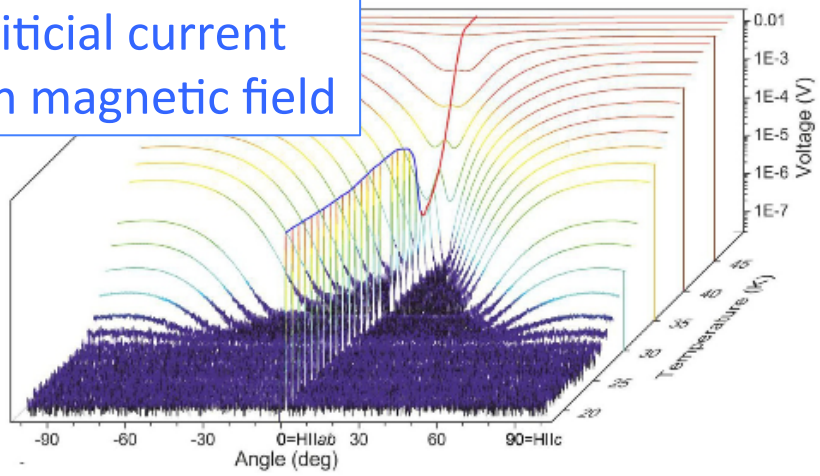

Moll, Batlogg et al

Opportunities – this is just the beginning

Structured samples

SmFeAs(O,F)

Focussed Ion Beam

Criticial current in magnetic field

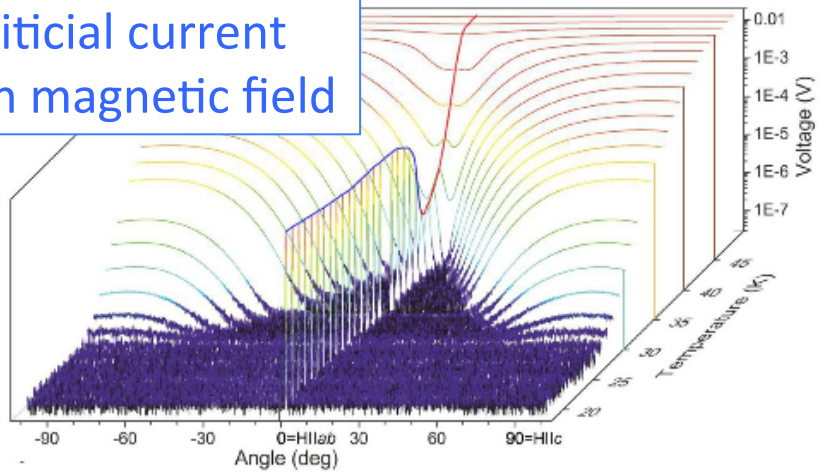

Moll, Batlogg et al

YBCO-LMO heterostructures

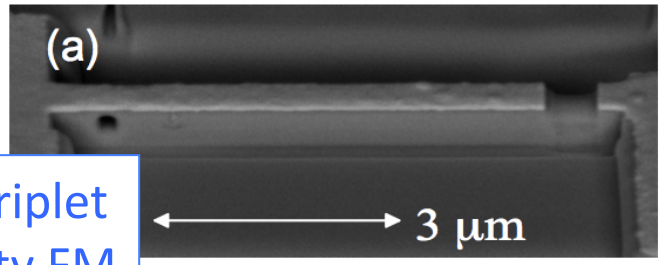

singlet-triplet proximity FM

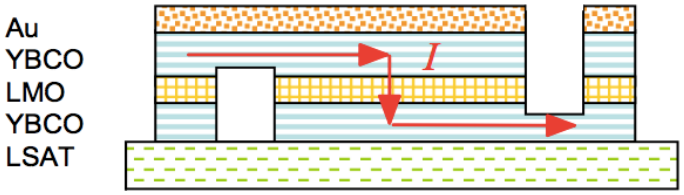

Krasnov & Bernhard groups

Opportunities – this is just the beginning

Structured samples

SmFeAs(O,F)

Focussed Ion Beam

Critical current in magnetic field

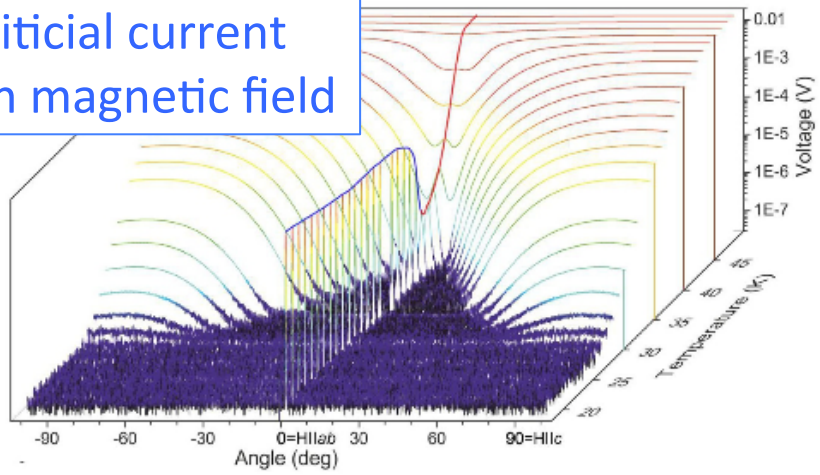

Moll, Batlogg et al

YBCO-LMO heterostructures

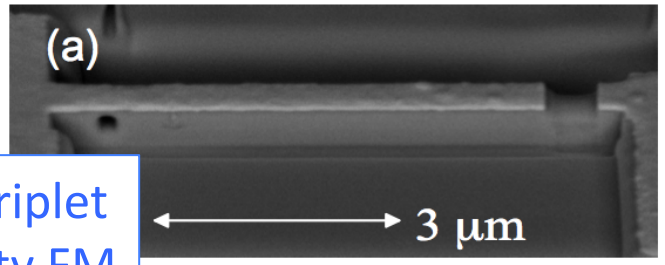

singlet-triplet proximity FM

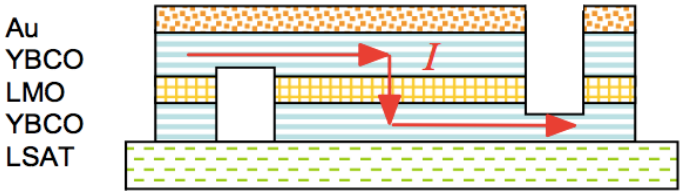

Krasnov & Bernhard groups

Little-Parks oscillations

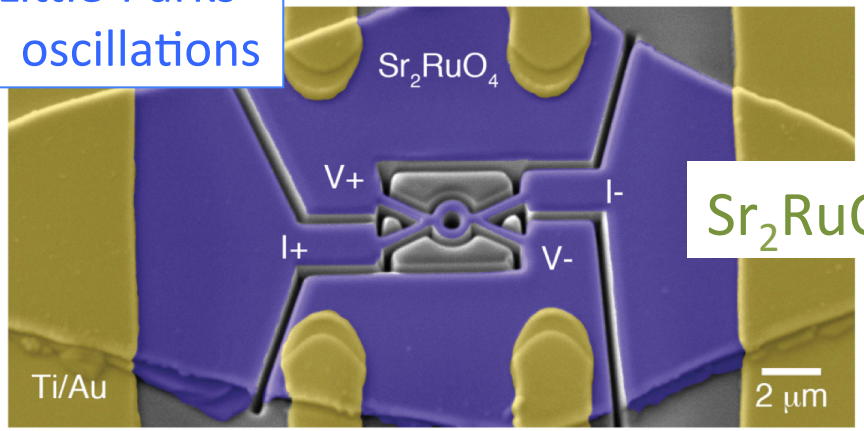

Sr_2RuO_4

Liu & Mao groups

$\Phi_0/2$ → *d*-textures ?